

NASA CR-140194

PROGRESS REPORT TO THE JOHNSON SPACE CENTER  
NATIONAL AERONAUTICS AND SPACE ADMINISTRATION  
FOR THE PERIOD ENDING JUNE 30, 1974

INTERACTION OF GASES WITH LUNAR MATERIALS

NASA Order T-9380A

Interagency Agreement 40-316-71

H. F. Holmes,<sup>1</sup> Principal Investigator  
E. L. Fuller, Jr.,<sup>1</sup> Co-Investigator  
R. B. Gammage,<sup>2</sup> Co-Investigator

<sup>1</sup>Chemistry Division  
<sup>2</sup>Health Physics Division  
Oak Ridge National Laboratory  
Post Office Box X  
Oak Ridge, Tennessee 37830

Operated by Union Carbide Corporation  
for the  
U.S. Atomic Energy Commission

(NASA-CR-140194) INTERACTION OF GASES  
WITH LUNAR MATERIALS Progress Report  
(Oak Ridge National Lab.) 64 p HC \$6.25

CSCCL 08H

63/06

Unclas  
48417

N74-32578



PROGRESS REPORT TO THE JOHNSON SPACE CENTER  
NATIONAL AERONAUTICS AND SPACE ADMINISTRATION  
FOR THE PERIOD ENDING JUNE 30, 1974

Contents

	<u>Page No.</u>
I. Introduction . . . . .	3
II. Materials and Experimental . . . . .	4
III. Results and Discussion . . . . .	5
A. Electron Microscopy . . . . .	5
B. Adsorption on an Apollo 11 Sample . . . . .	7
C. Porosity . . . . .	9
D. Reactivity with Water . . . . .	13
IV. Summary . . . . .	16
V. Work in Progress . . . . .	17
VI. Future Work . . . . .	17
VII. References . . . . .	18
VIII. List of Figures . . . . .	21
IX. Publications . . . . .	22

Note

This is a report of work in progress. Many of the numerical data and suggested interpretations printed are preliminary or tentative. Those wishing to use or quote such information are requested to consult the authors regarding final results and status of publication.

## I. Introduction

Sufficient experimental data dealing with the interaction of gases with lunar materials has now been accumulated so that one can describe, with a fair degree of confidence, the general surface characteristics of lunar fines. The most interesting of these general features is the manner in which water interacts with lunar fines. The reaction with water converts non-porous lunar fines into porous particles and, in the process, increases the specific surface area by a factor of two to three. These physical changes have been documented by measuring the adsorption of inert gases (e.g. nitrogen) before and after the reaction with water(1).

We have advanced the hypothesis that these physical changes result from the interaction of the adsorbed water film with latent damage tracks caused by energetic particles of solar or cosmic origin (1,2,3). If this is the case one might suspect a relationship between the water-induced porosity and the radiation history (e.g. exposure age) of the lunar samples. In addition, if the reaction with water is producing etched tracks such as those resulting from normal track etching experiments (4), these should be readily discernible from electron micrographs taken before and after the reaction with water.

This report is concerned with our continuing efforts to assess quantitatively the surface properties of lunar fines, particularly the water-induced porosity. Part of the report deals with additional interpretations of previously reported data (5). Some of the experimental work deals with a

clarification of a discrepancy in the preliminary results for the interaction of gases with lunar materials (6).

## II. Materials and Experimental

The specific samples discussed in this report are 10084,66; 63341,8; 74220,35 (the orange soil from Shorty Crater); and 74241,42 (the gray control soil). Sample 10084,66 was a reallocation of a returned sample. The sample history indicated that this aliquot had not suffered any deterioration except for exposure to the terrestrial atmosphere. The remaining three samples were normal allocations from NASA. Although these three samples were received in an atmosphere of dry nitrogen, exposure to the laboratory atmosphere was unavoidable during loading onto the two vacuum microbalance systems (7,8) used to obtain the data. Sample 74220,35 was unsieved while particles greater than one mm had been removed (by sieving) from the other three samples. 400-mg aliquots of each sample were used for the adsorption experiments. Because the specific surface area was generally less than one  $\text{m}^2/\text{g}$  great care must be exercised in determining background correction curves for each adsorbate as well as in the measurement of the actual isotherm (1). During the course of measuring an isotherm the error in weight measurement was normally within two micrograms. The resulting specific surface area uncertainty is about  $0.02 \text{ m}^2/\text{g}.$

High voltage electron micrographs of selected particles from sample 63341,8 were kindly provided by the group of M. Maurette in France. Scanning electron micrographs were obtained with existing equipment in the Analytical Chemistry Division of ORNL.

### III. Results and Discussion

#### A. Electron Microscopy

The high voltage electron micrographs in Figure 1 (taken by M. Maurette and J. P. Bibring) are three sub-micron sized particles from lunar fines sample 63341,8. Each of these particles had been subjected to a different pretreatment (see List of Figures). From the gas adsorption experiments pretreatments A(2) and C (see Section III.D.) gave non-porous particles while pretreatment B(2) gave porous particles. There are no readily visible differences in the three particles of Figure 1 that could be attributed to the different pretreatments. Maurette (9) and Bibring (10) looked at numerous particles from these three aliquots of 63341,8 and were unable to detect any changes. Maurette (9) and Bibring (10) conclude, and we agree, that the particles of 63341,8 are typical of a mature soil, have a high density of latent damage tracks, and that these damage tracks have clearly not been etched (in the normal sense) by the water treatments. It is worth mentioning that normal track studies, using strong etching conditions, produce etched tracks in the micron sized range (4). The largest dimension of the water-induced pore system, as deduced from the gas adsorption isotherms, is at least two orders of magnitude smaller than this.

Irrespective of whether the adsorbed water film is removing material from damage tracks or not, these results clearly demonstrate the ability of gas adsorption studies to sense physical characteristics and changes which are difficult, if not impossible, to study by other methods.

From previous results (5) it is known that the Apollo 17 orange soil (74220) develops a pore system and the specific surface area triples after exposure to water vapor at saturation vapor pressure. The reduction in the mean equivalent particle size is from 4.8 to 1.5 microns. Cadenhead (11,12,13) has postulated that the changes induced in lunar fines by exposure to high relative pressures of water vapor are due to a fracturing process. If adhering particles have been prised apart or particles fractured by the adsorbed water then changes in the particle size distribution should be observed in the scanning electron microscope. If, on the other hand, the expansion of surface area is internal (caused, for example, by dissolution of material along radiation damage tracks with formation of fine capillaries), the changes will not be visible in the microscope. Scanning electron micrographs were taken at 10,000 and 500 magnifications to observe particle sizes in the sub-micron and micron size ranges, respectively. Fines from the orange soil (74220) were examined before and after the water vapor treatment which induced the porosity (5). The scanning electron micrographs shown in Figure 2 reveal the predominantly glassy nature of the particles in the orange soil. Particles in the various size ranges were counted and their frequency of occurrence is given in Table I. No changes in the particle size distribution are

discernible. This result lends weight to the belief that the expansion of specific surface area is due to internal processes. The fracture hypothesis advanced by Cadenhead (12) is not of major significance in this case. Obviously the appearance of the particles is unaffected by the water vapor treatment; 80-85% of the particles are  $\leq 2$  microns in diameter with 75% of these lying in the size range of 0.1-0.5 micron.

#### B. Adsorption on an Apollo 11 Sample

Our preliminary results (6) for the adsorption of inert gases on the Apollo 11 soil 10087 were highly unique. We have indicated (1) that these preliminary results were probably erroneous because of failure to apply some critical blank corrections. As a result of this discrepancy NASA has provided us with an aliquot of the Apollo 11 sample 10084 (specifically 10084,66). The only difference in 10084 and 10087 is in the initial processing at the Lunar Receiving Laboratory (14). Since the specific aliquot of 10087 had been exposed to the terrestrial atmosphere for several months prior to use it is our contention that these two samples are identical.

Adsorption isotherms of the "inert" gases nitrogen, argon, carbon monoxide, and oxygen at 77°K (-196°C) are shown in Figure 3. Prior to these measurements, the sample was outgassed at 300°C, the same pretreatment used in the preliminary measurements. Figure 3 can be contrasted with Figure 1 of the preliminary results (6). The adsorption isotherms of Figure 3 are

much more "normal" and very similar to our results obtained for all other samples (1,2,5) we have studied except 10087. A BET treatment of the adsorption data for these four gases gave a specific surface area of  $0.50 \pm 0.05 \text{ m}^2/\text{g}$ . This is in general agreement with reported values [e.g., (2)] for other lunar fines but is much less than the preliminary value (6) of  $1.15 \text{ m}^2/\text{g}$  for 10087.

Following an additional outgassing at  $300^\circ\text{C}$ , sample 10084 was subjected to an adsorption-desorption cycle in water vapor at  $20^\circ\text{C}$ . The results of this experiment are shown in Figure 4, which can be contrasted with Figure 2 of the preliminary results (6) obtained with sample 10087. Conspicuously absent in Figure 4 are the sharp vertical steps at relative pressures of 0.9 and 0.8 in the adsorption and desorption data, respectively. Again the data in Figure 4 are quite similar to that observed for lunar fines other than 10087, e.g. 12001 and 63341 (2). In agreement with the "normal" behavior of lunar fines there was extensive retention of water ( $0.39 \text{ mg/g}$ ) on evacuation at the conclusion of the adsorption-desorption cycle.

The preliminary results (6) with sample 10087 indicated that the interaction with water vapor did not produce any significant change in the adsorptive capacity for nitrogen. This is in direct contrast to our results with all succeeding samples. To check on this anomaly, nitrogen adsorption (at  $77^\circ\text{K}$ ) on sample 10084 was measured after the reaction with water vapor. Isotherms for two outgassing temperatures are shown in Figure 5. These results clearly show that the sample has been significantly altered by the



reaction with water vapor. In particular, the specific surface area has increased from 0.50 to 0.94 m<sup>2</sup>/g after outgassing at room temperature with a further increase to 1.24 m<sup>2</sup>/g after outgassing at 300°C. In addition the sample now has a pore system which gives rise to a well-defined capillary condensation hysteresis loop in the adsorption-desorption isotherm. Furthermore, irreversibly adsorbed water remaining on the sample after outgassing at room temperature has a blocking effect on the access of nitrogen to the pore system. All of these results are in agreement with the general surface characteristics of other lunar fines (1,2,3,5).

We are forced to conclude that the preliminary results (6) obtained with sample 10087 are anomalous and should not be considered in any discussion of the surface characteristics of lunar samples or in any theories concerning the origin and history of the moon. In a general way, the surface properties of Apollo 11 fines seem to be quite similar to those of fines from the Apollo 12, 14, 16, and 17 missions. (We have not studied any fines from the Apollo 15 mission.) The anomalous isotherms for the inert gases on 10087 can be readily attributed to our failure to apply blank corrections to the data. However, the anomalous water isotherms remain unexplained at the present time.

### C. Porosity

Knowing that the reaction with water vapor creates a pore system in lunar fines, it is desirable to have some concept of the dimensions of the pores. This section deals with a semi-quantitative analysis of the nitrogen adsorption data to give an estimate of the pore sizes and their distribution.

The presence of micropores (these are defined as pores less than  $20\text{\AA}$  in diameter and which fill and empty reversibly at pressures less than that required for completion of the first physically adsorbed layer of nitrogen) was detected by a comparison method which is a variation of the "t-plot" method developed by de Boer (15). In essence the adsorption data are plotted as a function of the thickness of an adsorbed film of nitrogen (at the same pressure) on a reference non-porous solid. The choice of the reference isotherm is crucial but need not be discussed here. In some cases we have used an internal standard, i.e., nitrogen adsorption data taken on the same lunar sample under study but taken before the reaction with water. In several cases an internal standard is not possible because of the sequence of experiments. This does not seem to be critical as nitrogen adsorption (on a unit area basis) on lunar fines before the reaction with water is not highly dependent on the specific sample involved (3).

An example of such a comparison plot is shown in Figure 6. In this case the experimental sample is 63341 (2) outgassed at  $300^{\circ}\text{C}$  after the reaction with water vapor while the reference data is nitrogen adsorption on 12070 (1) outgassed at  $300^{\circ}\text{C}$  before the reaction with water. The intercept of the straight line at zero thickness gives the quantity of nitrogen adsorbed in micropores, which is usually converted to an equivalent micropore area,  $S_m$ . The slope of the straight line is a measure of the open area plus the area contained in larger pores and is designated as  $S_t$ . The sum of  $S_t$  and  $S_m$  should equal the area,  $S_{\text{BET}}$ , derived from a BET treatment of the nitrogen adsorption data on the experimental sample. In

the present case, the difference is 8% which is acceptable in view of the assumptions involved.

Dimensions and the size distribution of the larger pores have been estimated by application of the Kelvin equation to the nitrogen adsorption data. In view of the uncertainties attending the use of the Kelvin equation to calculate pore sizes and the undoubtedly complex nature of the pore system induced in the lunar fines, a simple procedure (16) which avoids excessive refinements has been adopted to measure the pore size distribution.

One of the parameters resulting from a Kelvin equation calculation is the cumulative pore volume. Figure 7 is an example of cumulative pore volume results. The specific lunar sample in this example is the Apollo 17 gray soil 74241. The nitrogen isotherms from which Figure 7 was calculated have been published (5). The most important feature of Figure 7 is the marked increase in pore volume available to nitrogen when irreversibly adsorbed water is removed by outgassing at 300°C. This result, the blocking of pore volume by irreversibly adsorbed water, has been observed for every lunar fines sample we have studied, although the amount of such blocking action depends on the specific sample and perhaps on the nature of the water treatment.

More interesting from a geometrical view is the pore size distribution resulting from a Kelvin treatment of the nitrogen sorption data. Figure 8 is, again, an example of two pore size distribution results. In this case the specific samples are the Apollo 17 orange and gray soils,

74220 and 74241, respectively. The results in Figure 8 were calculated from nitrogen adsorption data (5) taken after the samples had reacted with water. In both cases the samples were outgassed at 300°C and were, therefore, relatively free of irreversibly adsorbed water. The pore size distributions for these two samples are quite similar, with a fairly sharp peak at a Kelvin pore radius of about 24Å. The chief difference is that the orange soil (74220) has a larger contingent of pores having this dimension. One is lead to conclude that the water-induced pore structures of these two samples are quite similar even though the samples are markedly different in such factors as chemical composition, mineralogy, and exposure history (17).

An additional parameter resulting from porosity analysis is the cumulative area,  $\Sigma AS_p$ , of the walls of the pores. Although this involves some simple assumptions there should be a semi-quantitative relationship to the normal BET area,  $S_{BET}$ . Table II is a summary of the porosity analysis based on the comparison plots and also on calculations based on the Kelvin equation. Results from the comparison plot analyses are quite good in all cases ( $S_t + S_m$  is approximately equal to  $S_{BET}$ ). In considering the results from the Kelvin equation calculations we have assumed that the usual area,  $S_{BET}$ , contains three components:  $S_m$ , the equivalent area of micropores;  $S_o$ , the open surface which we have taken to be the area of the non-porous particles, as measured by nitrogen adsorption, before the reaction with water; and  $\Sigma AS_p$ , which is the area contained in pores

of radii  $\geq 20\text{\AA}$ . On this basis, the sum of these three components should be equal to  $S_{\text{BET}}$ . The results are not as good as those based on the comparison plot analysis but, considering the uncertainties and assumptions involved, they are quite consistent. The two worst cases are the low temperature outgasings of the Apollo 17 gray soil 74241. Even in this case the agreement is as good, or better than, many of the results based on much more highly refined methods. A complete discussion of Table II is outside the scope of the present report but certainly the most striking feature is the general similarity of the results for all four samples.

#### D. Reactivity with Water

All of the lunar fines that we have studied have reacted with water vapor at high relative pressures. The reaction with water vapor increases the specific surface area and creates a pore system. It was felt that the maximum alteration of lunar fines by reaction with water could be achieved by the simple expedient of soaking a sample in liquid water. To provide a useful comparison the sample should be one whose vapor phase reaction with water has been studied. Accordingly an aliquot of sample 63341,8, whose surface properties are known (2), was soaked in liquid water (while exposed to the laboratory atmosphere) for 30 days. The sample was then allowed to air-dry at room temperature to a constant weight prior to placing it in the vacuum microbalance system.

Nitrogen adsorption, at 77°K, was measured on this water-soaked sample after outgassing at 25 and 300°C. The resulting isotherms are shown in Figure 9 (pretreatment 1). Much to our surprise, the nitrogen isotherms

were completely reversible with no indication of hysteresis corresponding to capillary condensation in a pore system. In addition the specific surface areas, 0.51 and 0.57 m<sup>2</sup>/g, were only slightly increased from the original value of 0.42 m<sup>2</sup>/g (2). After again outgassing the sample at 300°C, water was forcibly condensed on the sample at 25°C (pretreatment 2 of Figure 9) in the absence of air. Subsequent nitrogen adsorption isotherms (after outgassing the sample) showed a drastic change in the adsorptive properties of this sample (Figure 9). All of the "usual" changes associated with water reacted lunar fines are now evident, including a capillary condensation hysteresis loop and a dramatic increase in the specific surface area to 0.99 m<sup>2</sup>/g with a further increase to 1.27 m<sup>2</sup>/g on outgassing at 300°C. The mild sintering on outgassing at 500°C (the specific surface area decreased to 1.10 m<sup>2</sup>/g) is comparable to that observed for Apollo 12 sample (2).

Exposure to air before and during the contact with liquid water has obviously blocked the alteration reaction. The subsequent reaction in the absence of air (Figure 9) cannot be attributed to outgassing at an elevated temperature (300°C) as the specific sample is known to react with saturated water vapor after outgassing at only 25°C (2), although the alteration is much less drastic. Experience with the Apollo 11 sample 10084 demonstrated that even small quantities of air will block the alteration reaction with water. During the first water adsorption cycle with this sample a leak in the system resulted in the accumulation of about one torr of air before reaching water saturation pressure. Subsequent nitrogen adsorption, after

outgassing showed that there had been very little, if any, change in the surface properties of the sample. However, a subsequent exposure to water vapor in the absence of air produced the "usual" results, i.e., a more than two-fold increase in specific surface area and the development of a pore system. The surface area changes are shown in Figure 10.

A logical, but not definitive, explanation for the blocking action of air is that some component of the terrestrial atmosphere is strongly adsorbed at the sites where attack by water occurs. The likely candidate is carbon dioxide but one cannot rule out oxygen or even nitrogen.

Figures 10 and 11 summarize the specific surface area data for these four samples of lunar fines. The figures are largely self-explanatory (see list of figures) but a few brief comments are worthwhile. The specific surface area is independent of the specific adsorbate used (Figure 10). Prior to alteration by reaction with water vapor the specific surface area is not very dependent on outgassing temperature. The opposite is true after the reaction with water and is due to the removal of irreversibly adsorbed water at the higher outgassing temperatures (5). The alteration of lunar fines is quite dependent on the manner in which the sample is exposed to water (results with 63341 in Figure 11). Results in Figures 10 and 11 are for lunar fines from three locations on the lunar surface. There is no correlation with location.

We have attributed the alteration of lunar fines by adsorbed water to an interaction of the sorbed water and latent damage tracks (1,2,3). The results (5) obtained with the Apollo 17 orange (74220) and gray (74241)

soils present an enigma in this respect. The orange soil, having a short exposure time (18), is one of the most reactive (toward water) of the samples we have studied. Recent information concerning damage tracks may be related to this problem. It has been found (19) that "young" tracks are different from "old" tracks, e.g. the etched length is longer for "young" tracks. It has also been shown (20) that irradiation with 3 MeV protons (about solar flare energy) markedly reduces the etchability of charged particle damage tracks. Both of these factors are probably involved in the water reactivity of the orange and gray soils from Apollo 17. We still believe that there is a relationship between radiation damage and the water reactivity of lunar fines, but a quantitative function can be defined only after conducting artificial high energy particle irradiations of annealed lunar fines and subsequent adsorptions of water.

#### IV. Summary

1. The changes induced in lunar fines are not visible in high energy electron micrographs.
2. Scanning electron micrographs have shown no change in particle size distribution as a result of the reaction with water.
3. From 1 and 2 above it is concluded that the water induced changes are internal to the particles themselves.
4. The surface properties of an Apollo 11 sample are similar to those of samples from the Apollo 12, 14, 16, and 17 missions. The preliminary results (6) for an Apollo 11 sample are anomalous.



5. A consistent analysis of the water induced porosity has been made in terms of microporosity, open area, and a distribution of pores which give capillary condensation (Kelvin behavior).

6. The normal laboratory atmosphere (or a component of it) blocks the alteration reaction with water.

7. The surface properties of mature lunar soils appear to be almost independent of chemical composition and mineralogy, but there are some variations in their reactivity toward water.

#### V. Work in Progress

Current experiments involve two aliquots of sample 63321 which have been outgassed at 400 and 700°C. Preliminary indications are that heating the sample to 700°C has markedly reduced the reactivity of the sample with adsorbed water, while heating to 400°C leaves the sample with "normal" reactivity. Most of the material in this report is being rearranged into a format suitable for publication in the open literature.

#### VI. Future Work

Some plans depend on results with sample 63321. If heating the sample at 700°C has eliminated or markedly reduced the alteration reaction with water we will attempt to restore the reactivity by irradiation with charged particles. The next sample we study will probably be 67481, a soil from North Ray Crater. These soils have been classed as immature and the results may provide a correlation of surface properties with soil maturity.

## VII. References

1. H. F. Holmes, E. L. Fuller, Jr., and R. B. Gammage, "Alteration of an Apollo 12 Samples by Adsorption of Water Vapor," Earth Plant Sci. Lett., 19, 90 (1973).
2. H. F. Holmes, E. L. Fuller, Jr., and R. B. Gammage, "Interaction of Gases with Lunar Materials: Apollo 12, 14, and 16 Samples," Proc. Fourth Lunar Sci. Conf., Geochim. Cosmochim. Acta, Suppl. 4, Vol. 3, 2413 (1973).
3. R. B. Gammage, H. F. Holmes, E. L. Fuller, Jr., and D. R. Glasson, "Pore Structures Induced by Water Vapor Adsorbed on Non-porous Lunar Fines and Ground Calcite," J. Coll. Interfac. Sci., 47, 350 (1974).
4. e.g., T. Pleininger, W. Kratschmer, and W. Genter, "Charge Assignment to Cosmic Ray Heavy Ion Tracks in Lunar Pyroxenes," Proc. Third Lunar Sci. Conf., Geochim. Cosmochim. Acta, Suppl. 3, Vol. 3, 2933 (1973).
5. H. F. Holmes, E. L. Fuller, Jr., and R. B. Gammage, "Some Surface Properties of Apollo 17 Soils," Proc. Fifth Lunar Sci. Conf., in press (1974). (A preprint of this paper was the progress report for the period ending January 31, 1974).
6. E. L. Fuller, Jr., H. F. Holmes, R. B. Gammage, and K. Becker, "Interaction of Gases with Lunar Materials: Preliminary Results," Proc. Second Lunar Sci. Conf., Geochim. Cosmochim. Acta, Suppl. 2., Vol. 3, 2009 (1971).

7. E. L. Fuller, Jr., H. F. Holmes, and C. H. Secoy, "Gravimetric Adsorption Studies of Thorium Dioxide Surfaces with a Vacuum Microbalance," Vac. Microbalance Tech., 4, 109 (1965).
8. E. L. Fuller, Jr., H. F. Holmes, R. B. Gammage, and C. H. Secoy, "Gravimetric Adsorption Studies of Thorium Oxide. IV. System Evaluation for High Temperature Studies," Prog. Vac. Microbalance Tech. (editors T. Gast and E. Robins), Heyden and Son, Ltd., New York, 1972, p. 265.
9. M. Maurette, personal communication (1973).
10. J. P. Bibring, personal communication (1974).
11. D. A. Cadenhead, N. J. Wagner, B. R. Jones, and J. R. Stetter, "Some Surface Characteristics and Gas Interactions of Apollo 14 Fines and Rock Fragments," Proc. Third Lunar Sci. Conf., Geochim. Cosmochim. Acta, Suppl. 3, Vol. 3, 2243 (1972).
12. D. A. Cadenhead and J. R. Stetter, "Terrestrial Atmosphere Weathering of Lunar Samples," Lunar Science V, The Lunar Science Institute, 1974, p. 103.
13. D. A. Cadenhead, J. R. Stetter, and W. G. Buerger, "Pore Structures in Lunar Samples," J. Coll. Interfac. Sci., 47, 322 (1974).
14. J. O. Annexstad, personal communication (1974).
15. e.g., B. C. Lippens and J. H. de Boer, "Studies on Pore Systems in Catalysts. V. The t-method," J. Catal., 4, 319 (1965).

16. S. J. Gregg and K. S. W. Sing, "Adsorption, Surface Area, and Porosity," Academic Press, London, 1967, Chapter 3.
17. Lunar Sample Preliminary Examination Team, "Apollo 17 Lunar Samples: Chemical and Petrographic Description," Science, 182, 659 (1973).
18. P. Eberhardt, O. Engster, J. Geiss, H. Graf, N. Grögler, S. Guggisberg, M. Jungck, P. Maurer, M. Märgeli, and A. Stettler, "Solar Wind and Cosmic Radiation History of Tarus Littrow Regolith," Lunar Science V, The Lunar Science Institute, 1974, p. 197.
19. G. Bastin, G. M. Comstock, J. C. Dran, J. P. Duraud, M. Maurette, and C. Thibaut, "Lunar Soil Maturation, Part III: Short-Term and Long-Term Aging of Radiation Damage Features in the Regolith," Lunar Science V, The Lunar Science Institute, 1974, p. 44.
20. S. A. Durrani, H. A. Khan, S. R. Malik, A. Aframian, J. H. Fremlin, and J. Tainey, "Charged Particle Tracks in Apollo 16 Lunar Glasses and Analogous Materials," Proc. Fourth Lunar Sci. Conf., Geochim. Cosmochim. Acta, Suppl. 4, Vol. 3, 2291 (1973).

### VIII. List of Figures

Figure 1. High voltage transmission electron micrograph of sub-micron particles from sample 63341,8. Pretreatment: A. Exposed to atmosphere only. B. Exposed to saturated water vapor in the absence of air. C. Soaked in liquid water (exposed to air) and air-dried.

Figure 2. Scanning Electron Micrographs of the orange soil (74220). A. Before water treatment (500X). B. After water treatment (500X). C. Before water treatment (10,000X). D. After water treatment (10,000X).

Figure 3. Adsorption of inert gases on Sample 10084,66 at 77°K (-196°C). Sample outgassed at 300°C. Measurements made before the reaction with water.

Figure 4. Adsorption of water on Sample 10084,66 at 20°C. Sample outgassed at 300°C.

Figure 5. Adsorption of Nitrogen on Sample 10084,66 at 77°K (-196°C). Measurements made after the reaction with water.

Figure 6. Comparison plot of nitrogen adsorption on Sample 63341 outgassed at 300°C after reaction with water. Reference data: Nitrogen adsorbed on 12070 outgassed at 300°C before reaction with water.

Figure 7. Cumulative pore volume ( $\Sigma \Delta V_p$ ) of the Apollo 17 gray soil (74241). Calculated from nitrogen sorption at 77°K (-196°C) after the reaction with water.

Figure 8. Pore size distribution ( $dV_p/dr_p$ ) for the Apollo 17 orange (74220) and gray (74241) soils. Calculated from nitrogen sorption at 77°K (-196°C) after the reaction with water. Samples outgassed at 300°C.

Figure 9. Nitrogen adsorption on Sample 63341,8 at 77°K (-196°C).

Figure 10. Specific surface area of Sample 10084 as measured by the adsorption of gases at 77°K (-196°C). Pretreatment: 1, before exposure to water at high relative pressures; 2, after exposure to water with little or no reaction at high relative pressures (air leak); 3, after reaction with water; 4, after accidental exposure to the laboratory atmosphere.

Figure 11. Specific surface areas as measured by the adsorption of nitrogen at 77°K (-196°C). Pretreatment: 1, before reaction with water; 2, soaked in liquid water for 30 days while exposed to the laboratory atmosphere; 3, exposed to saturated water vapor after evacuation at 25, 100, and 200°C; 4, after reaction with water.

#### IX. Publications

Two publications are attached.

1. "Interaction of Gases with Lunar Materials: Apollo 12, 14, and 16 Samples," Proc. Fourth Lunar Sci. Conf., Geochim. Cosmochim. Acta, suppl. 4, Vol. 3, 2413 (1973).

2. "Pore Structures Induced by Water Vapor Adsorbed on Non-porous Lunar Fines and Ground Calcite," J. Coll. Interfac. Sci., 47, 350 (1974).

A third publication, "Some Surface Properties of Apollo 17 Soils," has been accepted for publication in Proc. Fifth Lunar Sci. Conf. (A preprint of this paper was the progress report for the period ending Jan. 31, 1974).

Table I. Particle Sizes in the Orange Soil (74220) Before and  
After the Adsorption of Water Vapor

Particle Size Range (microns)	Frequency (%)	
	Before Water Treatment	After Water Treatment
- - - - From 500 magnification (Figure 2A and 2B) - - - -		
0.4 - 2	79	85
2 - 4	13	9
4 - 10	4	3
10 - 20	3	1
> 20	1	2
- - - - From 10,000 magnification (Figure 2C and 2D) - - - -		
0.02 - 0.1	13	11
0.1 - 0.2	30	28
0.2 - 0.5	42	43
0.5 - 1.0	15	18



Table II. Summary of Porosity Analysis of Nitrogen Sorption Data for  
Lunar Fines After the Reaction with Water

OGT <sup>a</sup>	$S_m$	$S_t$	$S_t + S_m$	$\frac{S_t + S_m}{S_{BET}}$	$S_{BET}$	$\frac{S_m + S_o + \Sigma \Delta S_p}{S_{BET}}$	$S_m + S_o + \Sigma \Delta S_p$	$\Sigma \Delta S_p$	$S_o^b$
----- 10084 -----									
25 <sup>c</sup>	0.19	0.77	0.96	1.02	0.94	1.19	1.12	0.43	0.50
300	0.38	0.96	1.34	1.08	1.24	1.21	1.51	0.63	0.50
----- 63341 -----									
25 <sup>c</sup>	0.09	0.90	0.99	1.00	0.99	1.02	1.01	0.50	0.42
300	0.38	0.99	1.37	1.08	1.27				
500	0.44	0.78	1.22	1.11	1.10				
----- 74220 -----									
25 <sup>c</sup>	0.17	0.73	0.90	0.99	0.91	1.13	1.03	0.50	0.36
100	0.19	0.84	1.03	1.01	1.02	1.06	1.08	0.53	0.36
200	0.26	1.17	1.43	1.02	1.40	0.94	1.32	0.64	0.42
300	0.23	1.18	1.41	1.02	1.38	0.99	1.37	0.72	0.42
----- 74241 -----									
25 <sup>c</sup>	0.16	0.47	0.63	1.11	0.57	1.46	0.83	0.31	0.36
100	0.20	0.51	0.71	1.11	0.64	1.42	0.91	0.35	0.36
200	0.18	0.75	0.93	1.06	0.88	1.11	0.98	0.44	0.36
300	0.27	0.82	1.09	1.08	1.01	1.08	1.09	0.46	0.36

<sup>a</sup>Outgassing temperature in °C.

<sup>b</sup>Open surface area. Taken equal to specific surface area before the reaction with water.

<sup>c</sup>Outgassed at room temperature.

Other symbols are defined in the text. All S values are in m<sup>2</sup>/g.

PHOTO 0611-74

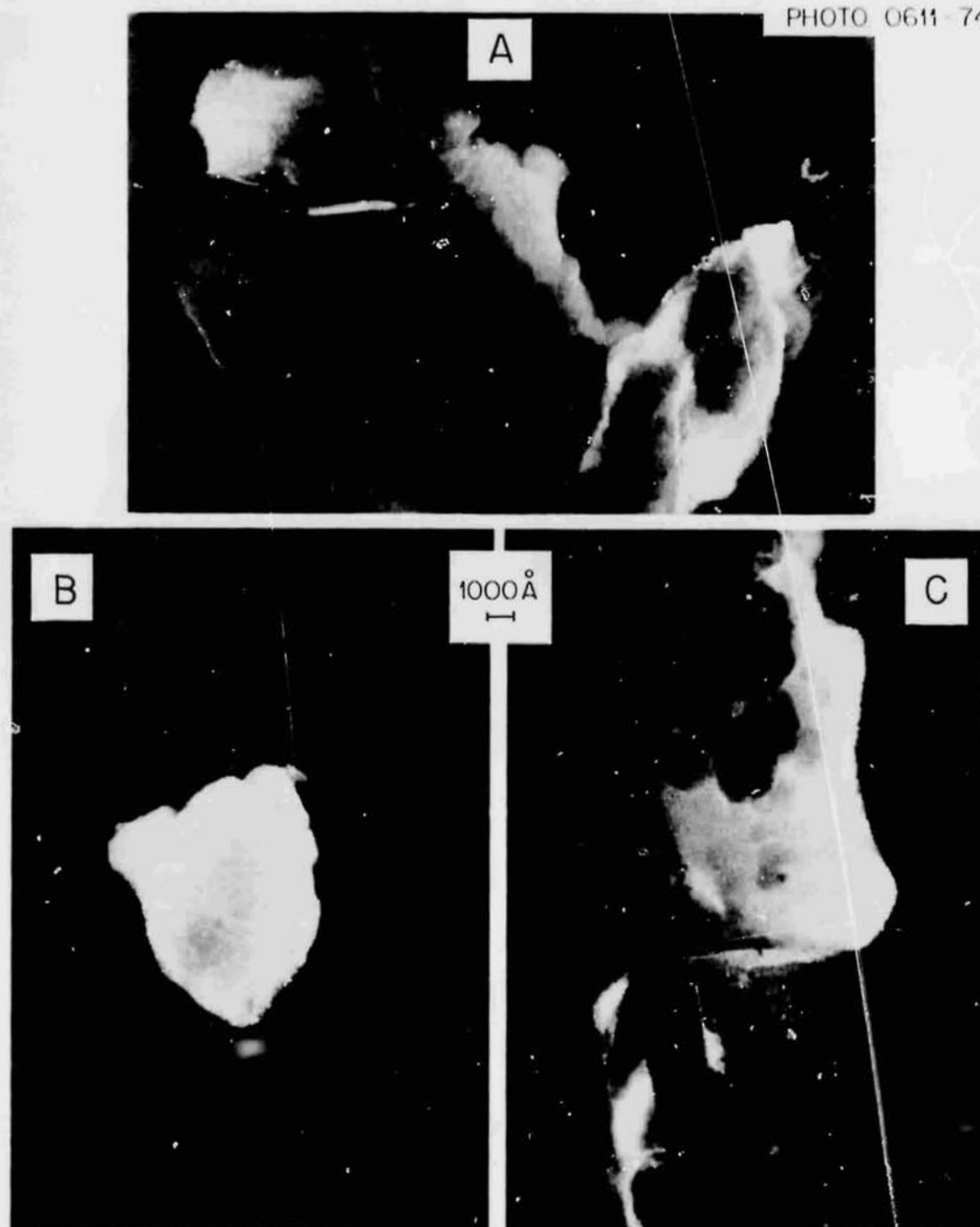


Fig. 1. High voltage transmission electron micrograph of sub-micron particles from sample 63341,8. Pretreatment: A. Exposed to atmosphere only. B. Exposed to saturated water vapor in the absence of air. C. Soaked in liquid water (exposed to air) and air-dried.

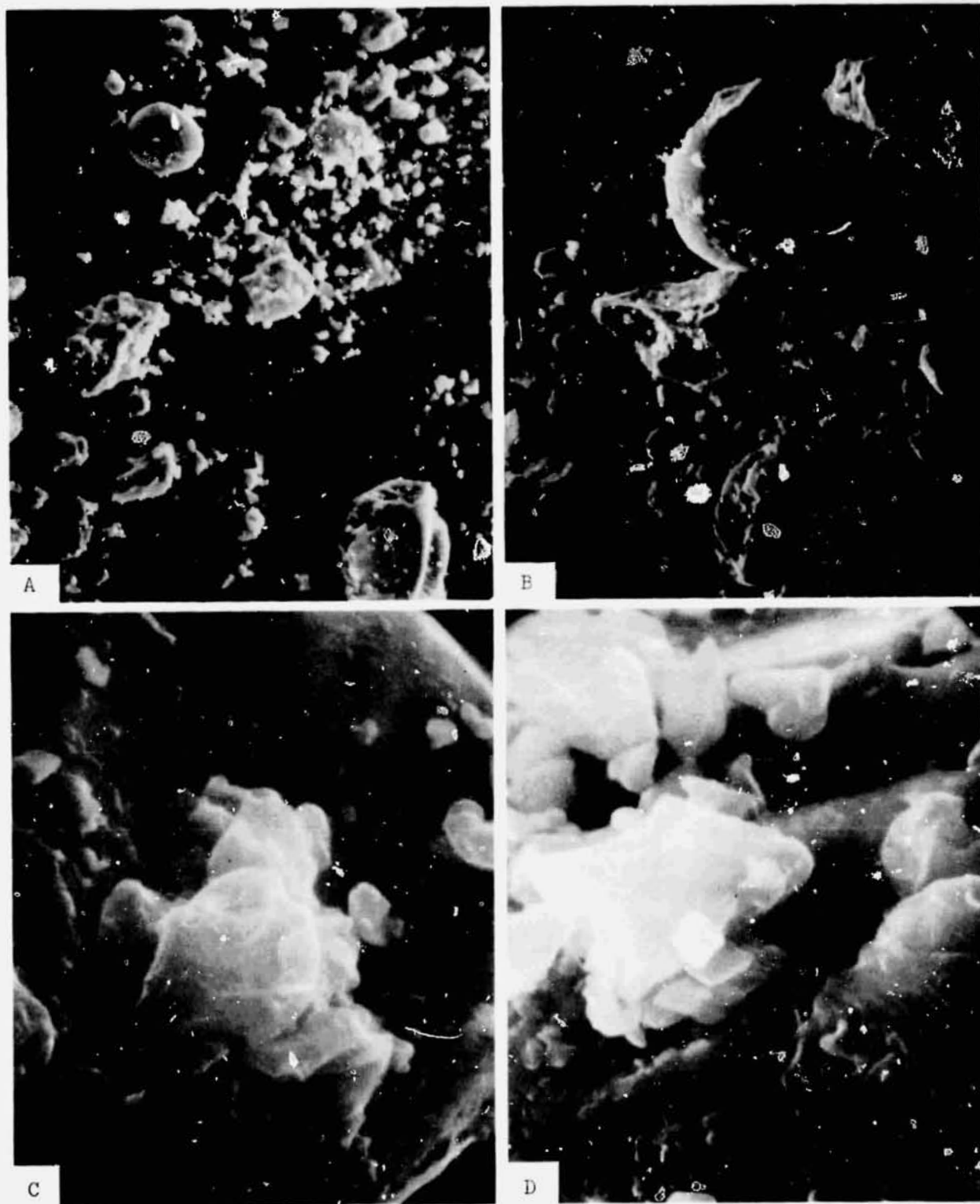


Fig. 2. Scanning electron micrographs of the orange soil (74220).  
A. Before water treatment (500X). B. After water treatment (500X).  
C. Before water treatment (10,000X). D. After water treatment (10,000X).

ORNL-DWG. 74-7140

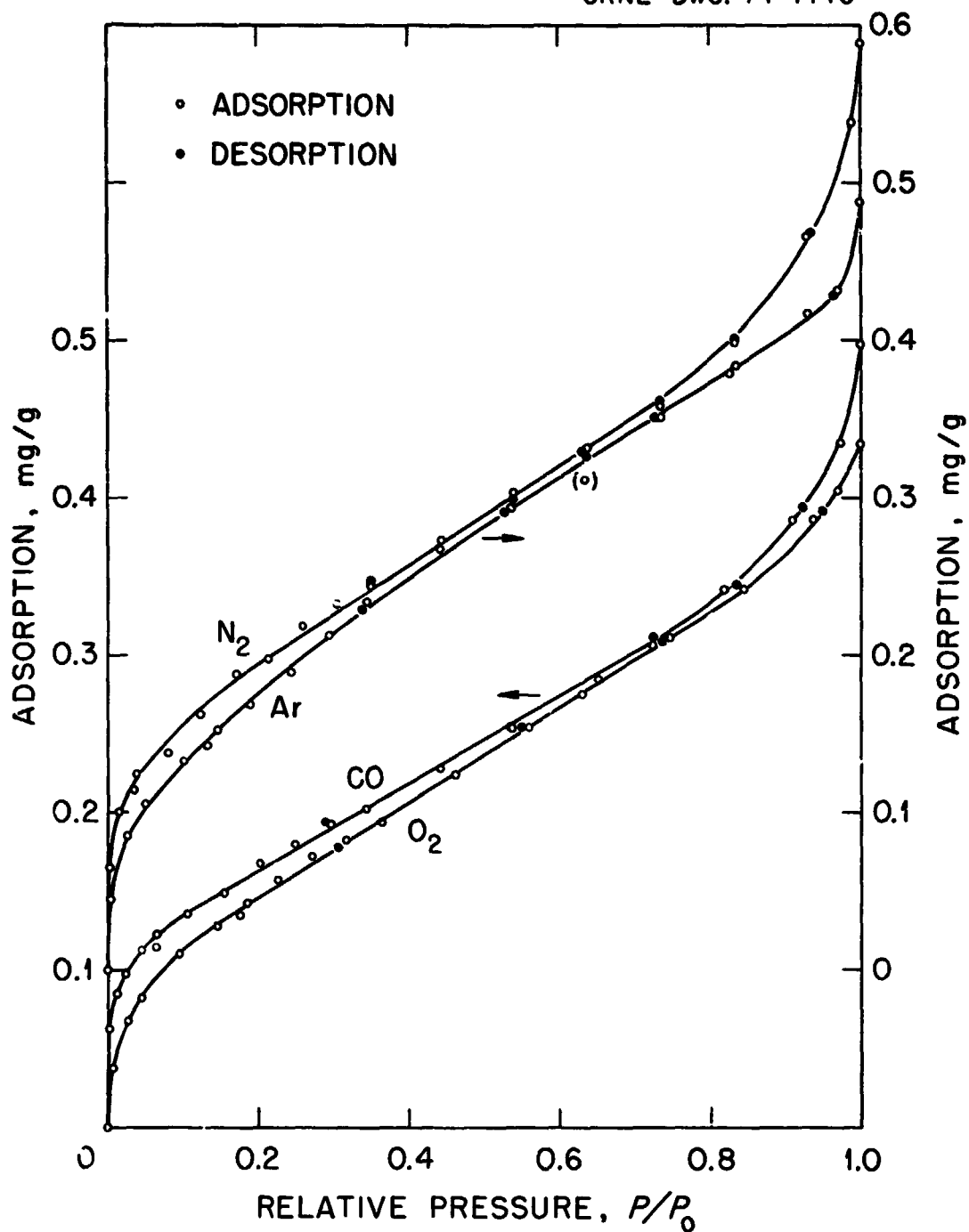


Fig. 3. Adsorption of inert gases on sample 10084,66 at 77°K (-196°C). Sample outgassed at 300°C. Measurements made before the reaction with water.

ORNL-DWG. 74-7141

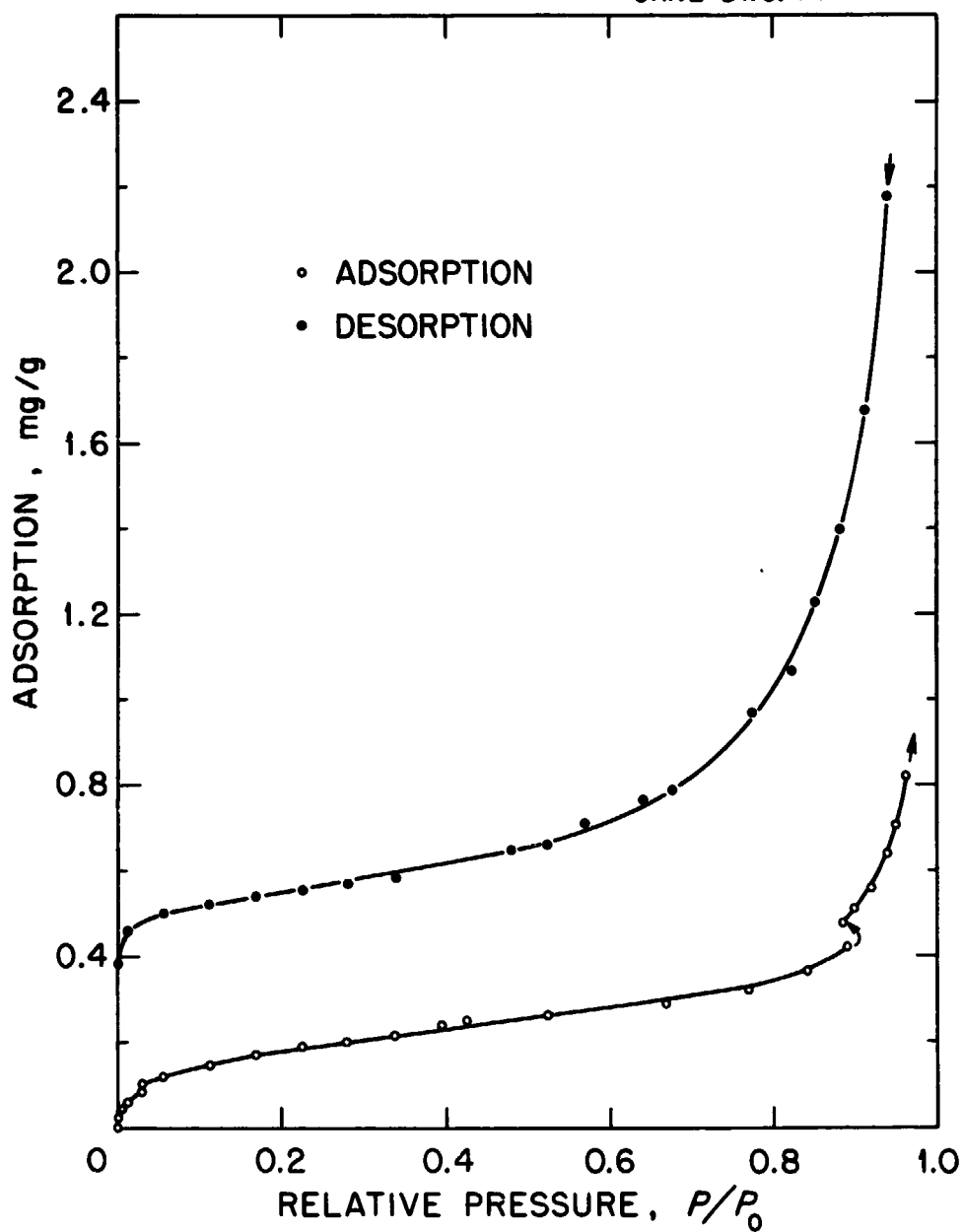


Fig. 4. Adsorption of water on sample 10084,66 at 20°C. Sample outgassed at 300°C.

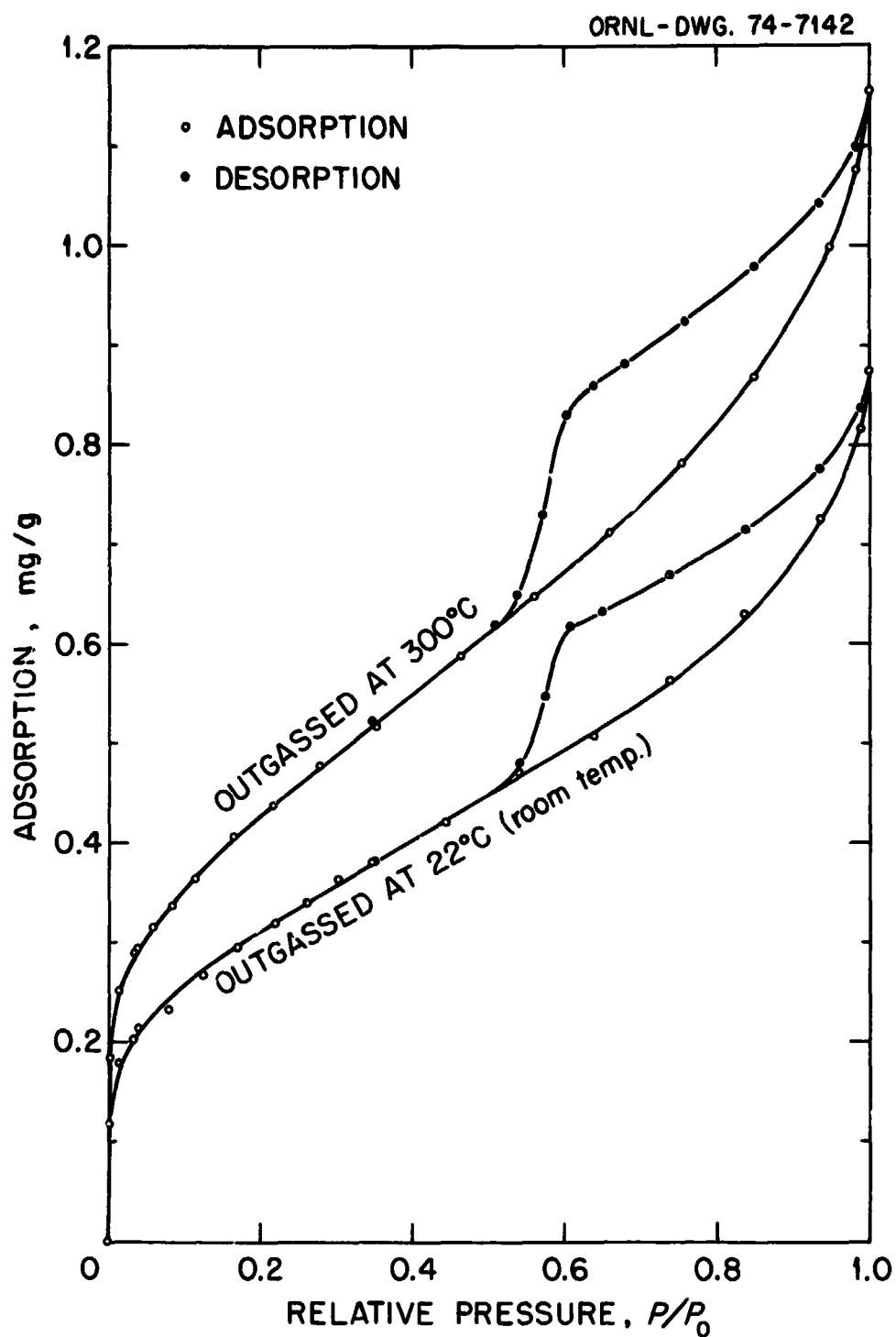


Fig. 5. Adsorption of nitrogen on sample 10084,66 at 77°K (-196°C). Measurements made after the reaction with water.

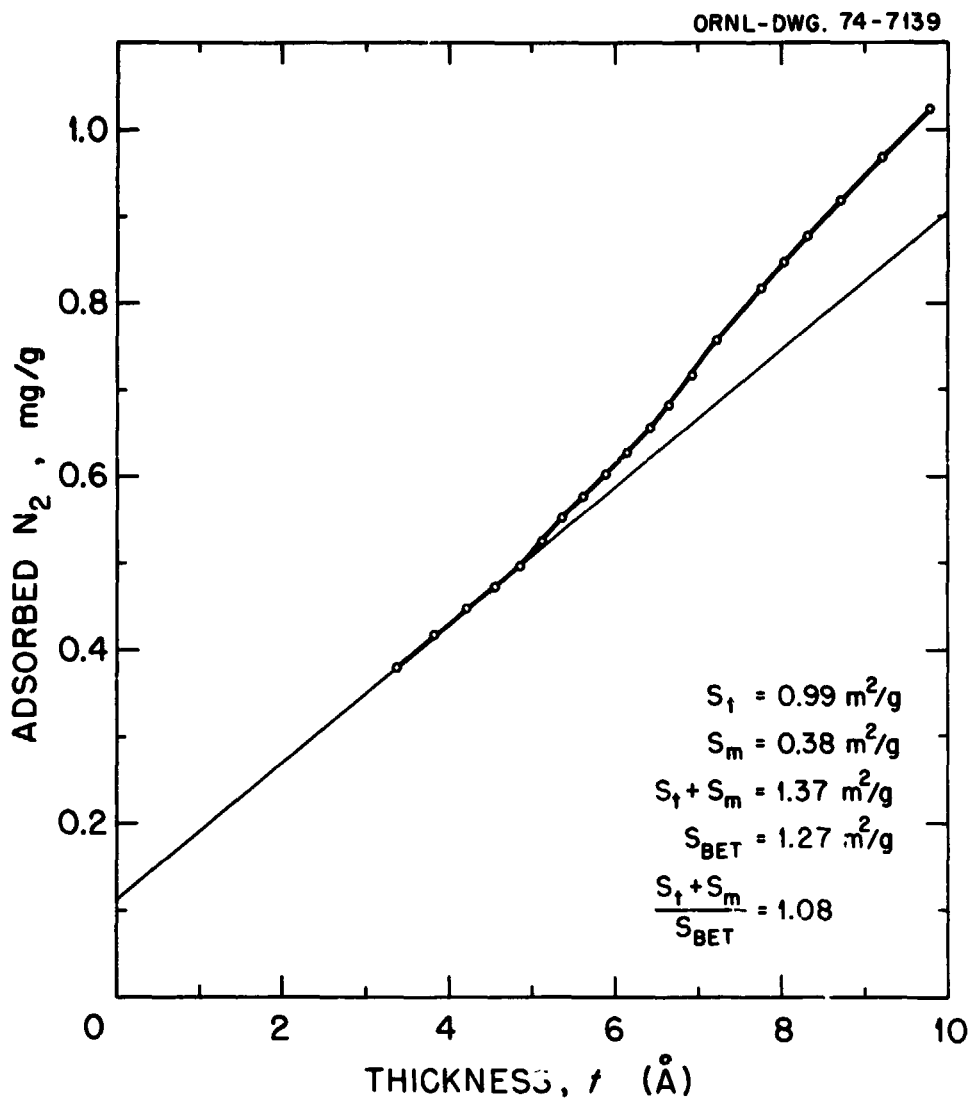


Fig. 6. Comparison plot of nitrogen adsorption on sample 63341 outgassed at 300°C after reaction with water. Reference data: Nitrogen adsorbed on 12070 outgassed at 300°C before reaction with water.

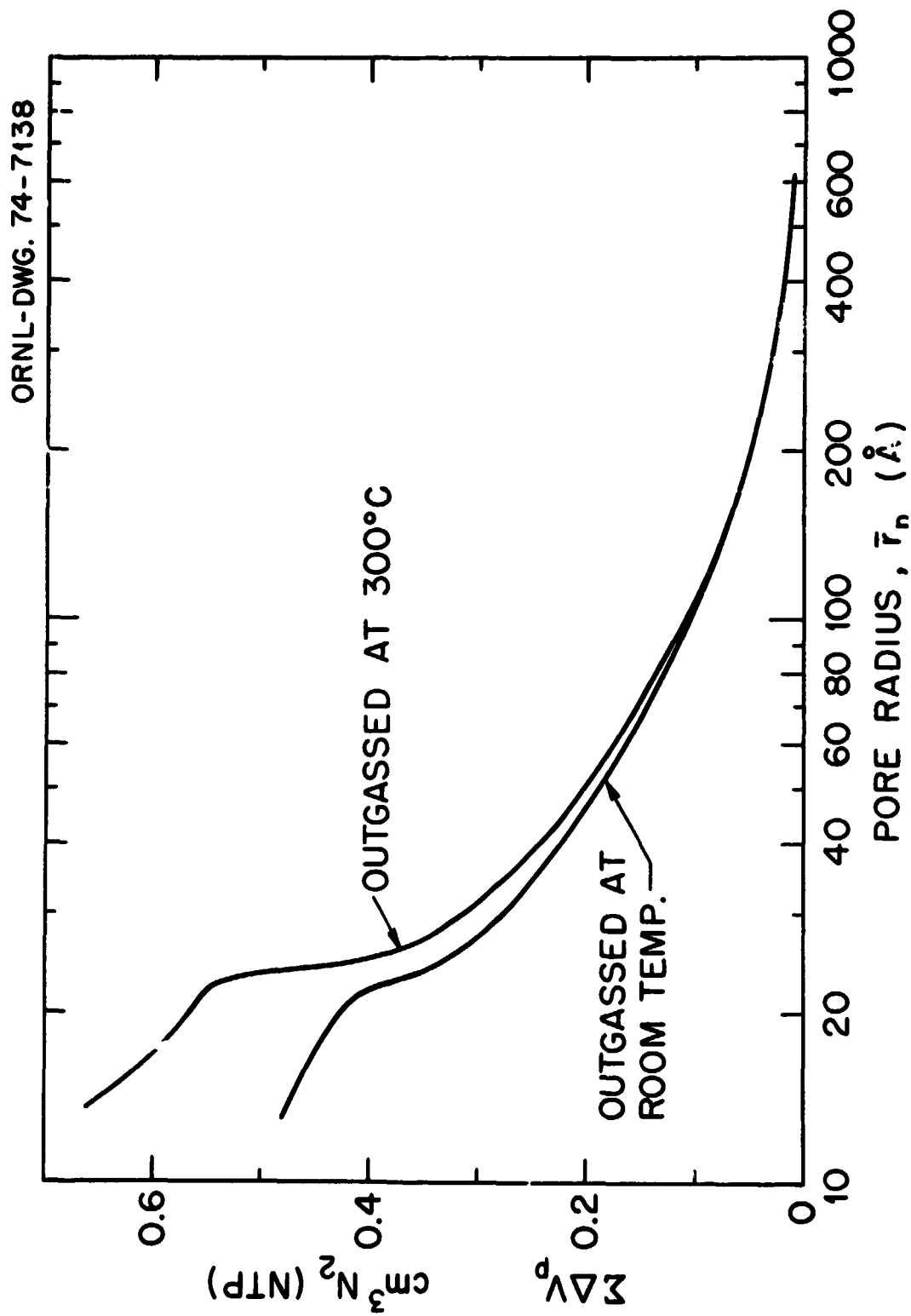


Fig. 7. Cumulative pore volume ( $\Sigma \Delta V_p$ ) of the Apolito 17 gray soil (74241). Calculated from nitrogen sorption at 77°K (-196°C) after the reaction with water.



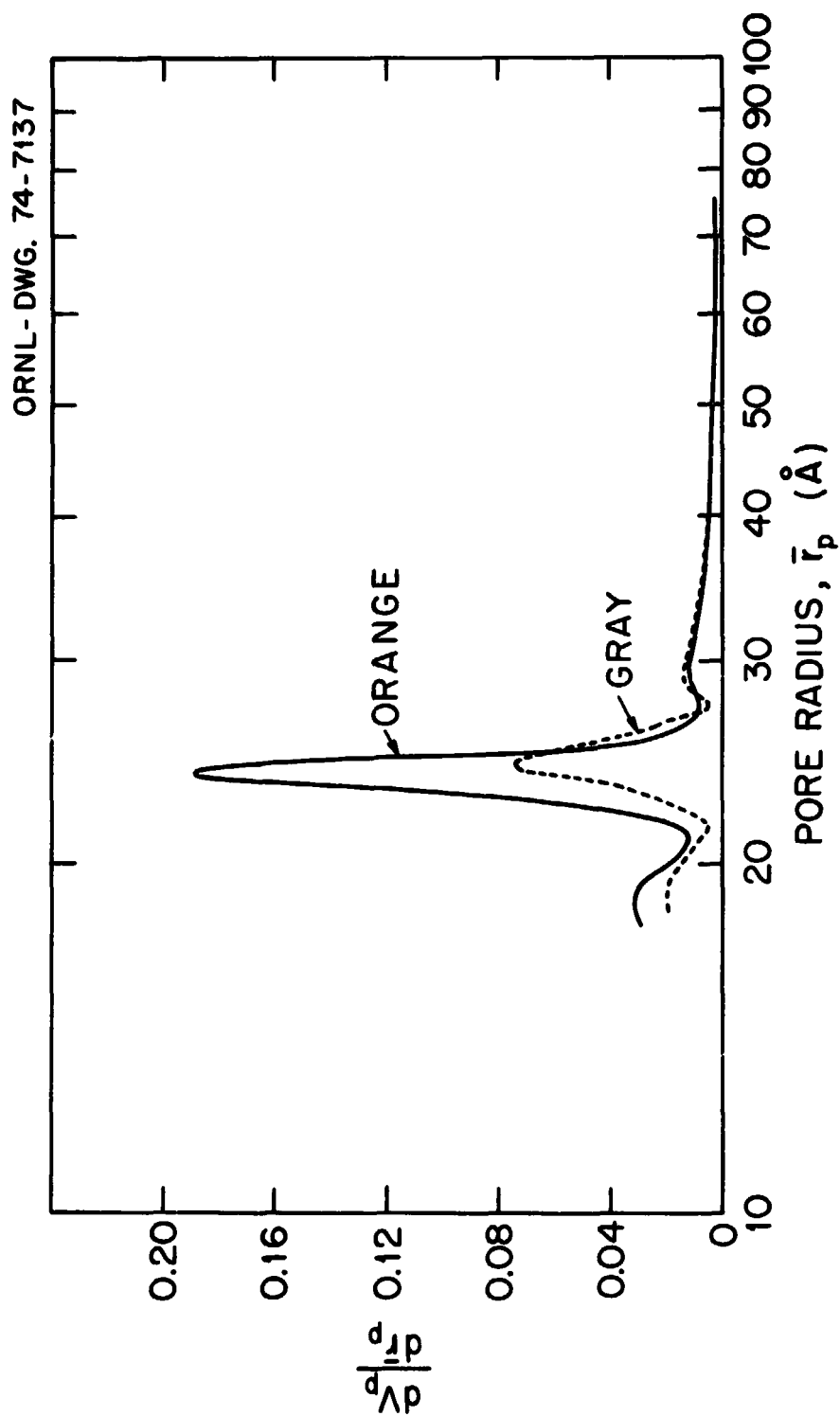


Fig. 8. Pore size distribution ( $dV_p/d\bar{r}_p$ ) for the Apollo 17 orange (74220) and gray (74241) soils. Calculated from nitrogen sorption at 77°K (-196°C) after the reaction with water. Sample outgassed at 300°C.

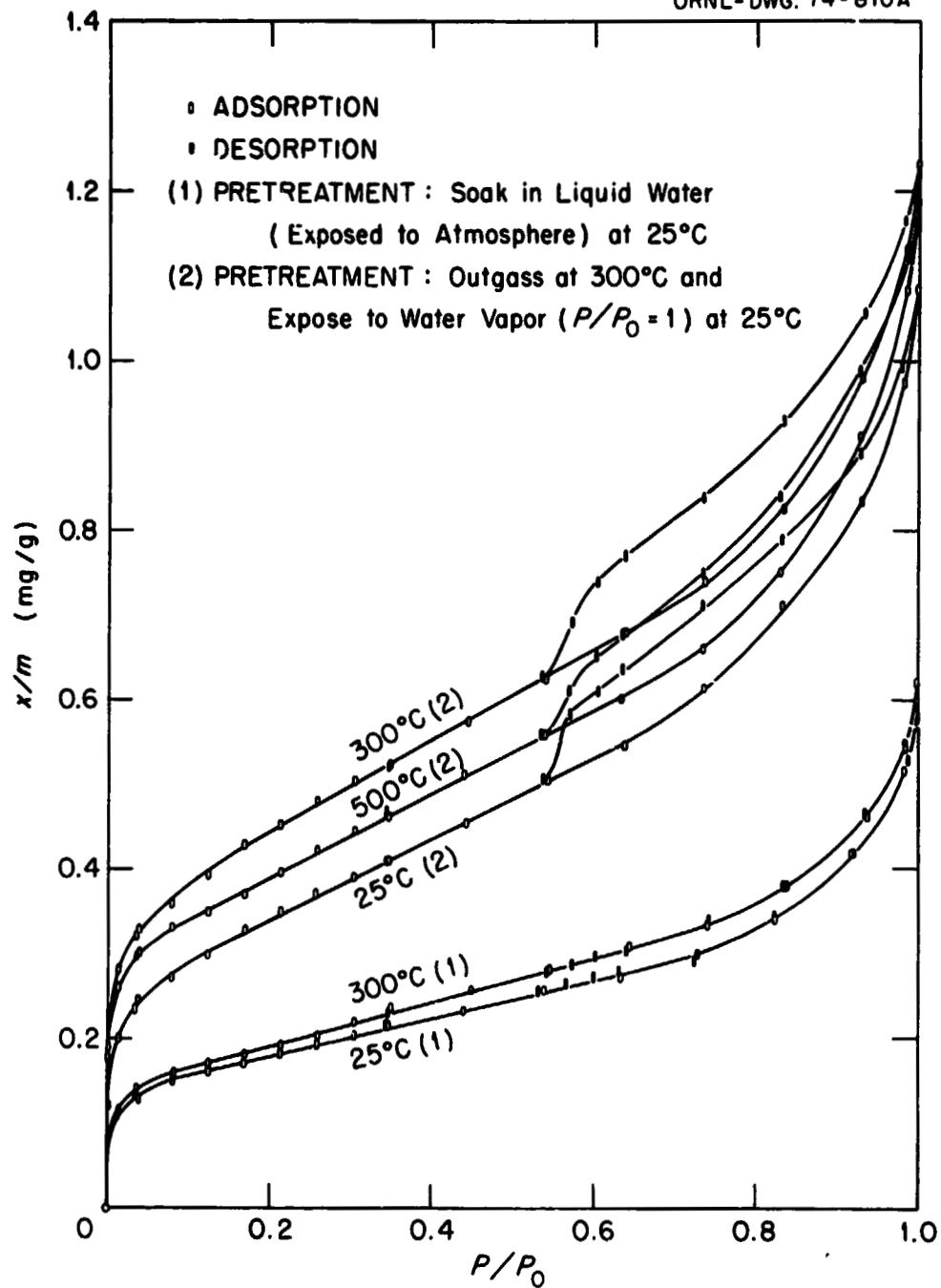


Fig. 9. Nitrogen adsorption on sample 63341,8 at 77°K (-196°C).

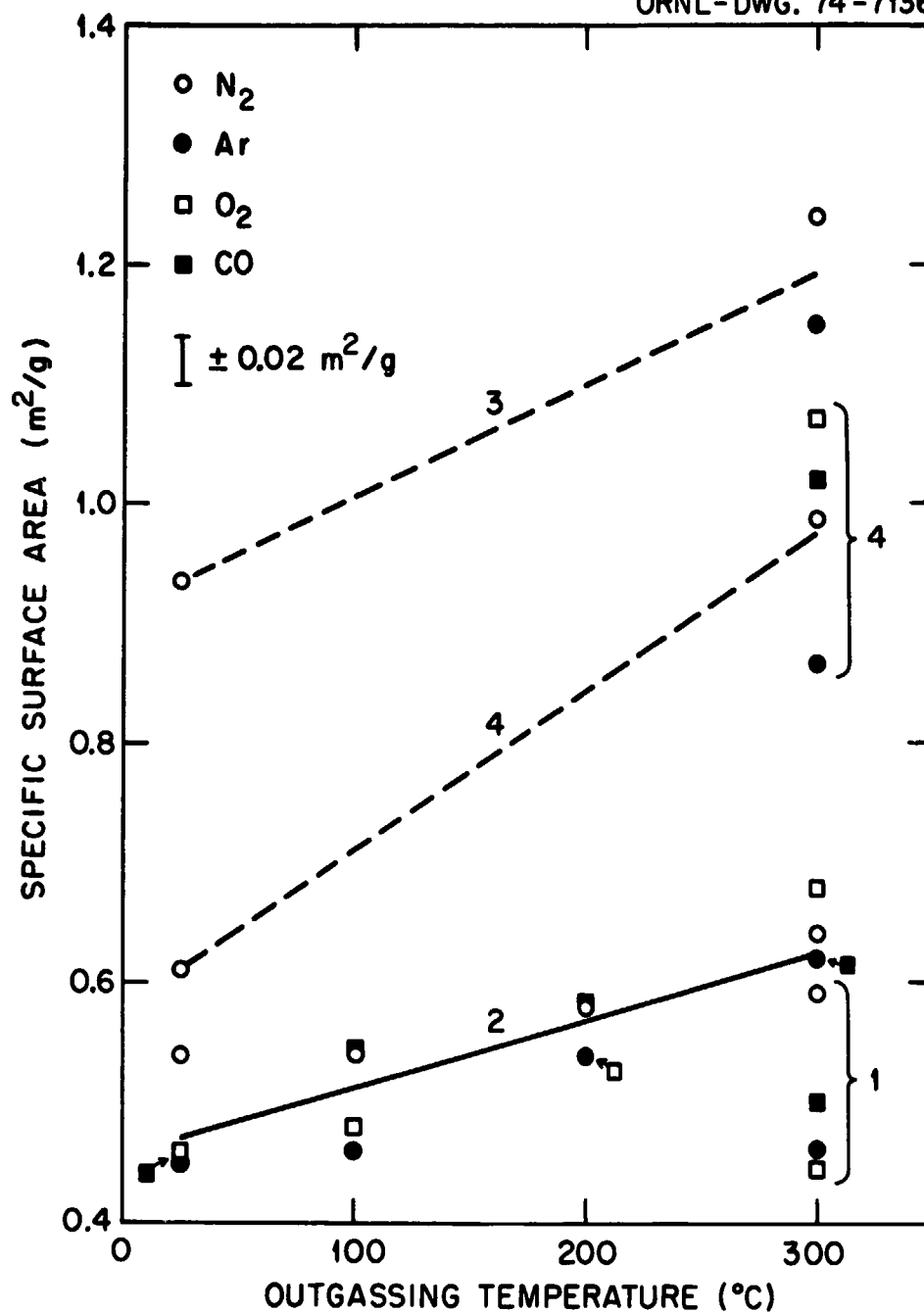


Fig. 10. Specific surface area of sample 10084 as measured by the adsorption of gases at  $77^{\circ}\text{K}$  ( $-196^{\circ}\text{C}$ ). Pretreatment: 1, before exposure to water at high relative pressures; 2, after exposure to water with little or no reaction at high relative pressures (air leak); 3, after reaction with water; 4, after accidental exposure to the laboratory atmosphere.

ORNL-DWG. 74-7135

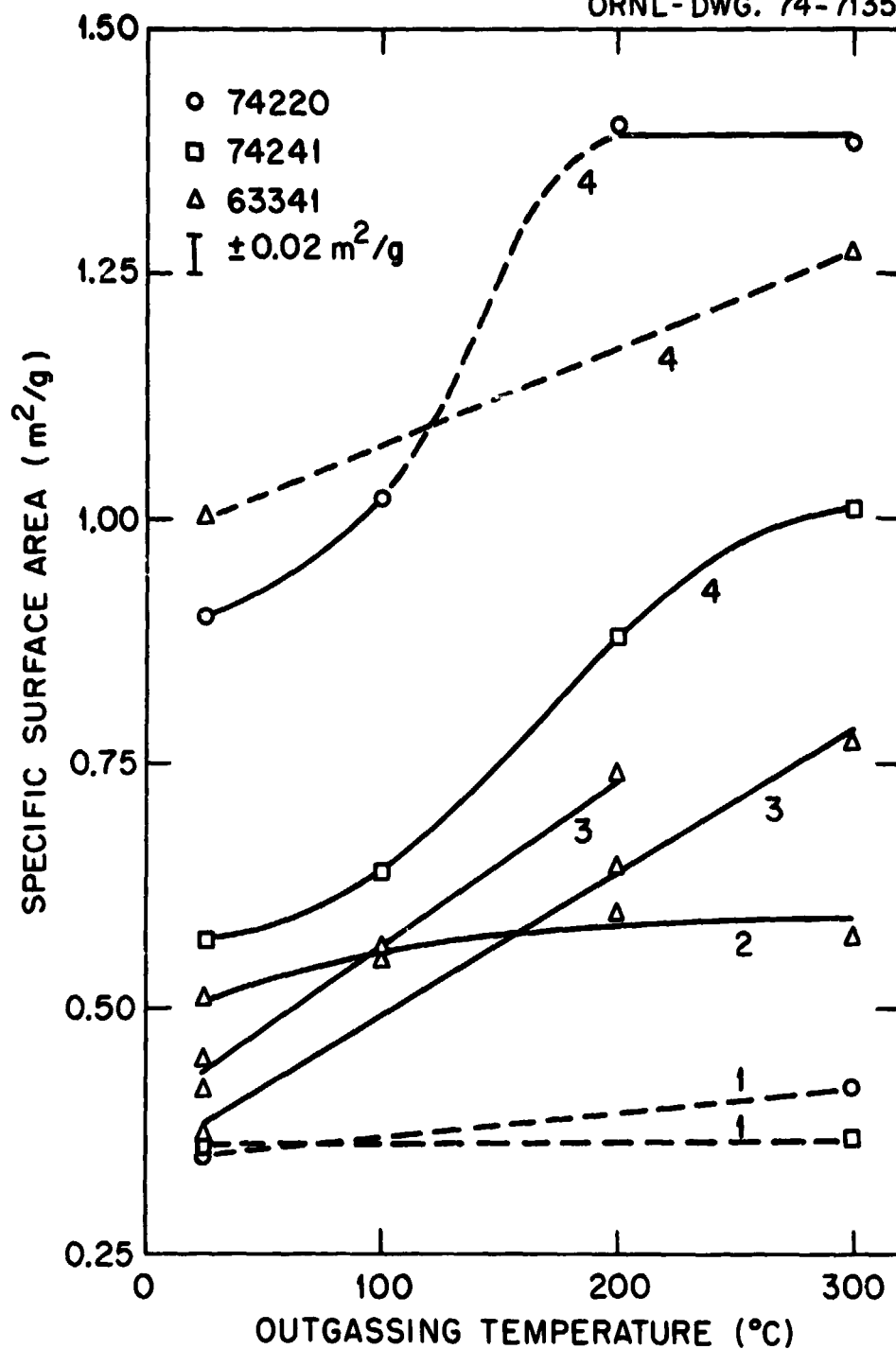


Fig. 11. Specific surface areas as measured by the adsorption of nitrogen at  $77^{\circ}\text{K}$  ( $-196^{\circ}\text{C}$ ). Pretreatment: 1, before reaction with water; 2, soaked in liquid water for 30 days while exposed to the laboratory atmosphere; 3, exposed to saturated water vapor after evacuation at 25, 100, and  $200^{\circ}\text{C}$ ; 4, after reaction with water.

**GEOCHIMICA ET COSMOCHIMICA ACTA**  
Journal of The Geochemical Society and The Meteoritical Society  
**SUPPLEMENT 4**

**PROCEEDINGS**  
**OF THE**  
**FOURTH LUNAR SCIENCE CONFERENCE**  
**Houston, Texas, March 5-8, 1973**

Sponsored by  
The NASA Johnson Space Center  
and  
The Lunar Science Institute



**PERGAMON PRESS**

Printed in the U.S.A.

## Interaction of gases with lunar materials: Apollo 12, 14, and 16 samples\*

H. F. HOLMES and E. L. FULLER, JR.

Reactor Chemistry Division  
Oak Ridge National Laboratory  
Oak Ridge, Tennessee 37830

R. B. GAMMAGE

Health Physics Division  
Oak Ridge National Laboratory  
Oak Ridge, Tennessee 37830

**Abstract**—Surface properties of lunar fines samples from the Apollo 12, 14, and 16 missions have been investigated by studying the adsorption of nitrogen, argon, oxygen, carbon monoxide (all at 77°K), and water vapor (at 20 or 22°C) on the samples. Initially the samples were all nonporous and had a uniformly low specific surface area (0.3 to 0.6 m<sup>2</sup>/g). Water interacts strongly with the surface of lunar fines, chemisorbing at low pressures followed by a massive adsorption at high pressures. Nitrogen adsorption measurements after the interaction with water showed the surface properties had undergone a severe alteration as a result of the attack by water vapor. This alteration consisted of a marked increase in the specific surface area and the creation of a pore system. The results are interpreted on the basis of a penetration of water into the damage tracks.

### INTRODUCTION

THE INTERACTION of gases with lunar particles provides information on surface characteristics at the molecular level of dimensions. The BET treatment (Brunauer *et al.*, 1938) of the adsorption data provides a quantitative measure of the specific surface area. In addition, if pores are present in sizes ranging up to a few hundred angstroms their size and distribution can be ascertained from the adsorption isotherms. No other reliable methods are available for characterizing pore structures in this size range (Gregg and Sing, 1967).

In addition to providing basic information concerning the state of subdivision of lunar soils and their porosity, the specific surface area is a quantitative measure of their capacity to adsorb reactive molecules (e.g., water and carbon dioxide) from an environment. Such information would, for example, be vital for the establishment of life support stations on the lunar surface. A more immediate problem is the possible weathering and deterioration of lunar samples by the terrestrial atmosphere. Lunar fines from the Apollo 11 and 12 missions have been shown to interact extensively with water vapor (Fuller *et al.*, 1971; Holmes *et al.*, 1973). It is important to determine if this strong interaction with water vapor is a general characteristic of lunar fines and to correlate the interaction with, for

\*Research sponsored by NASA under Union Carbide contract with the U.S. Atomic Energy Commission.

example, the radiation damaged nature of lunar materials. In general, the surface properties of lunar fines will have to be considered in theories concerning the formation and history of such samples.

#### EXPERIMENTAL

The adsorption-desorption measurements were made with existing vacuum microbalance systems which have been described in detail (Fuller *et al.*, 1965, 1972). Both systems were equipped with a device for maintaining a constant pressure of water vapor during equilibration at each chosen pressure (Fuller *et al.*, 1972). Background blank corrections have been applied to all of the data. These corrections, and their critical importance for accurate acquisition of adsorption data, have been discussed recently (Holmes *et al.*, 1973).

Experimental procedures were generally the same as we have used for our studies of adsorption on thorium oxide (Holmes *et al.*, 1968; Gammage *et al.*, 1972). Prior to an adsorption experiment each sample was always outgassed for a minimum of 16 hours (overnight). Outgassing pressures were in the range of  $10^{-4}$  to  $10^{-6}$  torr (measured on a 25 mm O.D. manifold leading directly to the balance chamber) and the temperatures ranged from 20 to 1000°C. Measurement of the isotherms required 15 to 20 minutes for equilibration at each pressure except for water vapor at high relative pressures which required an overnight waiting period, or longer, for equilibration.

Results reported in this paper were obtained with 0.3 or 0.4 g aliquots of lunar fines samples 12001,151, 12070,218, 14003,60, and 63341,8. These samples were the fine sieve fraction ( $< 1$  mm) of lunar soil and were used without further classification. When measuring adsorption at 77°K (liquid nitrogen bath) by gravimetric techniques it is necessary to apply a buoyancy correction to the data. In order to calculate this correction we have used the mean value ( $2.95 \pm 0.09$  g/cm<sup>3</sup>) of the reported densities (Greene *et al.*, 1971) of selected particles from Apollo 12 lunar fines. Weight determinations are estimated to be reliable to  $\pm 2$  micrograms over the extended time interval involved in the experiments.

#### RESULTS

Isotherms for the adsorption of carbon monoxide, at 77°K, on lunar samples 12001,151, 14003,60, and 63341,8 are shown in Fig. 1. The amount of adsorption, in mg of adsorbate per g of sample, is shown as a function of the relative pressure,  $P/P_0$ , where  $P_0$  is the saturation vapor pressure of carbon monoxide at 77°K. The shape of these isotherms is quite common and fits the general classification of Type II isotherms found for adsorption on nonporous solids (Brunauer, 1943). There was exact reversibility on desorption with no indication of hysteresis or other complicating factors. Isotherms for the adsorption of nitrogen, argon, and oxygen (all at 77°K) on these three lunar samples were near duplicates of the carbon monoxide isotherms.

It should be emphasized that all of the isotherms were completely reversible over the entire pressure range from high vacuum to saturation. All of the data for the adsorption of the four gases on these three lunar samples were subjected to a standard BET treatment (Brunauer *et al.*, 1938) to obtain monolayer capacities and "C" constants. Monolayer capacities were converted to specific surface areas by means of recommended cross-sectional areas (McClellan and Harnsberger, 1967) for the adsorbates (the values we have used are given in Table 1). Results from the BET treatment of the data are summarized in Table 1. Agreement of the specific surface areas should be tempered by the fact that cross-sectional areas for

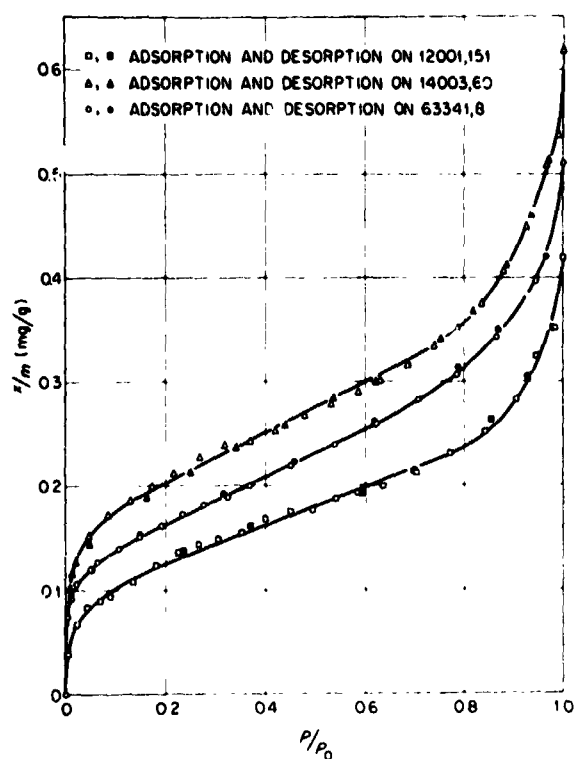


Fig. 1. Adsorption of carbon monoxide on lunar fines at 77°K. Samples outgassed at 25°C.

Table 1. Specific surface areas and BET "C" constants for lunar samples outgassed at 25°C.

Adsorbate	Sample 12001,151		Sample 14003,60		Sample 63341,8	
	$\Sigma$	C	$\Sigma$	C	$\Sigma$	C
N <sub>2</sub> <sup>a</sup>	0.33	65	0.51	84	0.42	57
Ar <sup>b</sup>	0.34	12	0.54	37	0.38	31
CO <sup>c</sup>	0.35	82	0.60	100	0.49	113
O <sub>2</sub> <sup>d</sup>	—	—	0.54	12	0.42	21

$\Sigma$  = Specific surface area in m<sup>2</sup>/g.

<sup>a</sup>Co-area = 16.2 Å<sup>2</sup>.

<sup>b</sup>Co-area = 16.6 Å<sup>2</sup> and  $P_0$  is that of supercooled liquid.

<sup>c</sup>Co-area = 16.8 Å<sup>2</sup>.

<sup>d</sup>Co-area = 17.5 Å<sup>2</sup>.



adsorbed molecules are usually selected to give agreement with nitrogen adsorption data. For example, the range of values commonly used for oxygen is 14 to 18 Å<sup>2</sup> (Gregg and Sing, 1967). If these co-areas are applied to the oxygen data for sample 14003,60 the resulting range of specific surface area is 0.43 to 0.56 m<sup>2</sup>/g which is still reasonable agreement. The BET "C" constant is a measure of the average net heat of adsorption for about the last half of monolayer completion (Brunauer, 1961), that is, for adsorption on the least energetic sites on the surfaces of the lunar particles.

Without outgassing the samples at an elevated temperature water vapor isotherms were measured at 20 or 22°C on these same lunar samples. The complete isotherm for 63341,8 and the adsorption data for 12001,151 are shown in Fig. 2. A characteristic feature of all water isotherms which we have measured on lunar fines is a general hysteresis over the entire pressure range including vacuum retention (irreversibly adsorbed water which could not be removed by prolonged evacuation at the conclusion of the isotherm).

An additional common feature is the massive adsorption of water vapor at high relative pressures (above 0.9). Specific surface areas calculated from the water

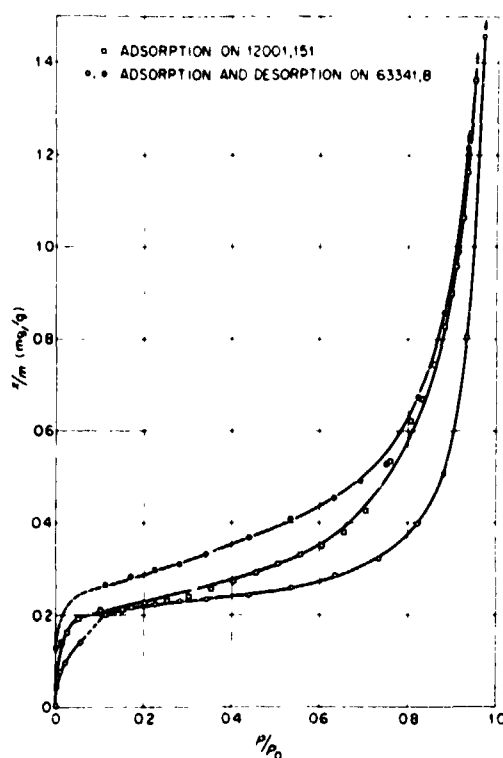


Fig. 2. Adsorption of water vapor on lunar fines. Samples outgassed at 20°C (63341,8) and 22°C (12001,151). Isotherms measured at these respective temperatures.

data are uncertain because of the general irreversibility of the isotherms coupled with the specific nature of water adsorption (this latter factor gives rise to a large uncertainty in the cross-sectional area of an adsorbed water molecule). However, a visual comparison of the disparity between the adsorption and desorption branches of the water isotherms (e.g., sample 63341,8 in Fig. 2 and Holmes *et al.*, 1973) indicates that the capacity for reversible physical adsorption of water has increased as a result of the adsorption-desorption cycles.

After several additional adsorption-desorption cycles in water vapor the adsorption of nitrogen (at 77°K) on these samples was remeasured. Figure 3 shows nitrogen adsorption on sample 12001,151 before and after the water adsorption experiments. Supporting experiments with samples not treated with water vapor have shown that the changes were brought about by the action of water vapor and not by raising the outgassing temperature from 25 to 300°C. Corresponding nitrogen adsorption isotherms for lunar sample 63341,8 are shown in Fig. 4. As a result of the water treatment the amount of nitrogen adsorption is greater at all pressures and the isotherms have well defined hysteresis loops at relative pressures above 0.5. The specific surface area of sample 12001,151 increased from 0.33 to 0.97 m<sup>2</sup>/g because of exposure to water vapor during the adsorption experiments. The corresponding increase for sample 63341,8 is from 0.42 to 0.74 m<sup>2</sup>/g. Results for sample 14003,60 are in essential agreement with the data presented in Figs. 3 and 4.

Nitrogen adsorption (at 77°K) on samples 12001,151 and 12070,218 was meas-

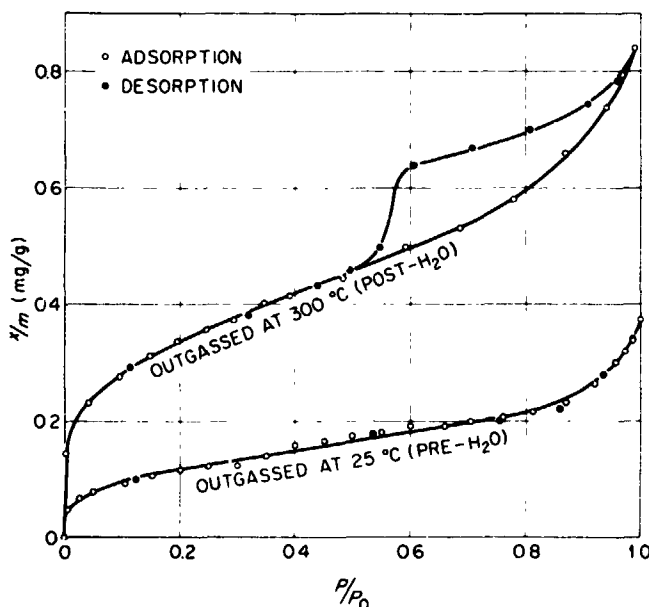


Fig. 3. Adsorption of nitrogen on 12001,151 at 77°K.

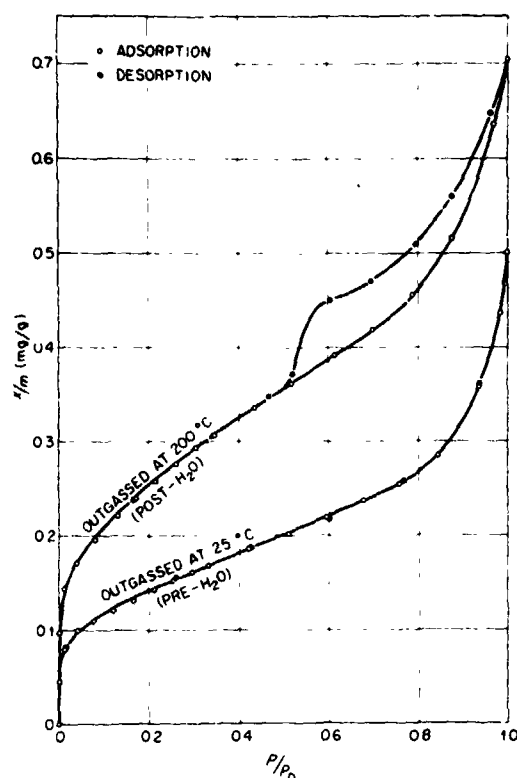


Fig. 4. Adsorption of nitrogen on 63341,8 at 77°K.

ured after outgassing the samples at increasing temperatures from 500 to 1000°C. The resulting isotherms are shown in Fig. 5 (for sample 12001,151) and Fig. 6 (for sample 12070,218). (For the sake of clarity no data points are shown for 12001,151 but the precision of the data is well within the estimated error bar shown on the isotherm which was measured after outgassing the sample at 800°C.) There is a general decrease in the amount of adsorption (at all pressures) as the outgassing temperature is increased. This decrease is reflected in the specific surface areas which are given in Table 2. The high pressure hysteresis loop induced by the reaction with water vapor was absent for samples 12070,218 and 12001,151 after outgassing at 700° and 800°C, respectively.

#### DISCUSSION

Data tabulated in Table 1 are in essential agreement with the uniformly low specific surface areas which have been reported for lunar fines samples (Fuller *et al.*, 1971; Holmes *et al.*, 1973; Cadenhead *et al.*, 1972; Grossman *et al.*, 1972). By assuming spherical or cubical particles one can calculate an effective particle size

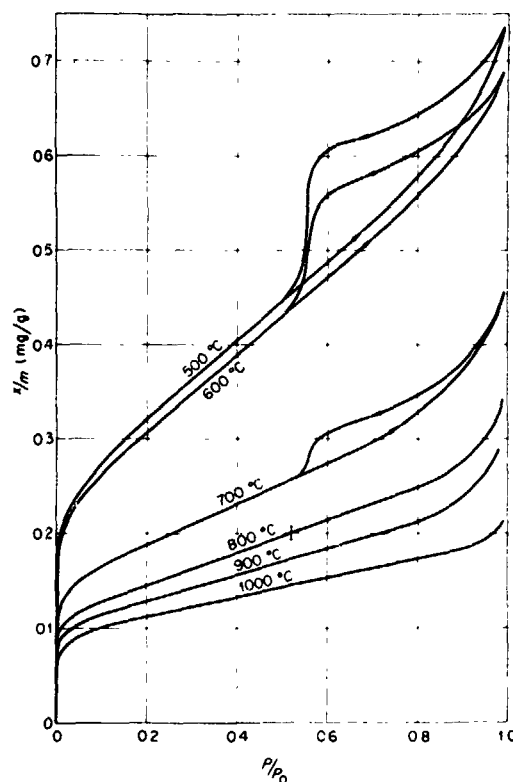


Fig. 5. Adsorption of nitrogen on 12001,151 at 77°K. Sample outgassed at indicated temperatures (Post-H<sub>2</sub>O).

Table 2. Specific surface area as a function of outgassing temperature.

Outgassing Temperature (°C)	Sample 12001,151 $\Sigma(\text{m}^2/\text{g})$	Sample 12070,218 $\Sigma(\text{m}^2/\text{g})$
500	0.90	1.15
600	0.87	—
700	0.52	0.59
800	0.42	—
900	0.37	0.49
1000	0.31	0.37

from the specific surface areas given in Table 1. Mean particle sizes calculated in this manner range from 3 to 6 microns. This is in reasonable agreement with particle sizes deduced from sedimentation studies (e.g., Gold *et al.*, 1972). Since sedimentation studies give the Stokes diameter for an equivalent sphere this agreement indicates the absence of gross surface roughness and/or internal area.

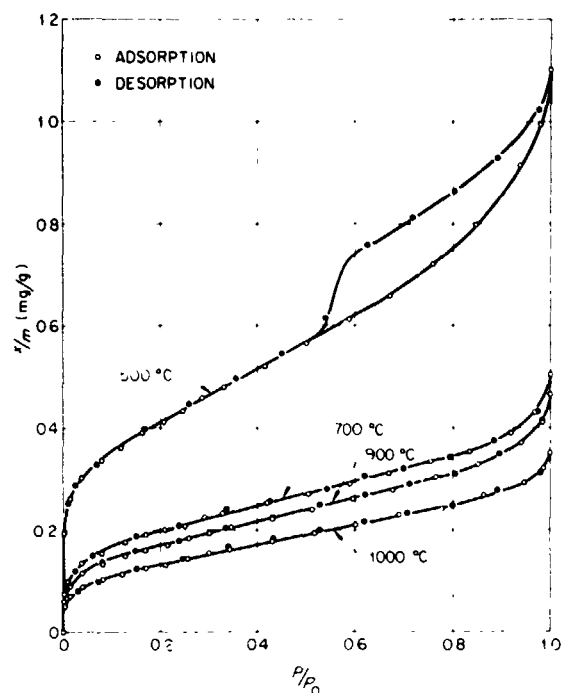


Fig. 6. Adsorption of nitrogen on 12070,218 at 77°K. Sample outgassed at indicated temperatures (Post-H<sub>2</sub>O).

Average net heats of adsorption calculated from the "C" constants given in Table 1 range from 380 ( $C = 12$ ) to 730 cal/mole ( $C = 113$ ). These values are in qualitative agreement with the expected trend based on polarizability, quadrupole, and dipole contributions to adsorption energies for these four adsorbates. This trend in adsorption energies has been observed for terrestrial materials such as titanium oxide (Smith and Ford, 1965).

The reversibility of the initial isotherms is a clear indication that these samples do not have the type of porosity which gives rise to capillary condensation hysteresis loops. It should be emphasized that we are referring to the porosity of individual soil particles and not, for example, to the type of porosity which results from the random packing of particles. In order to cause hysteresis effects in adsorption isotherms the pore size must be a few hundred angstroms or less (Gregg and Sing, 1967). Adsorption in larger pores is essentially like adsorption on open surfaces. These results, coupled with previous work (Fuller *et al.*, 1971; Holmes *et al.*, 1973), indicate that the approximate surface characteristics of lunar fines (prior to water treatment) are independent of their location on the lunar surface. Most probably there are processes occurring on the lunar surface to produce a lunar soil whose dynamic equilibrium properties include a relatively

low specific surface area coupled with a lack of porosity. These processes certainly include micrometeorite impact, solar wind sputtering, and radiation damage (e.g., Dran *et al.*, 1972; Phakey *et al.*, 1972).

The contrasting nature of water adsorption on these samples, as compared to adsorption of the "inert" gases, is evident from a comparison of Figs. 1 and 2. Retention of water in high vacuum and the low pressure hysteresis can be explained on the basis of chemisorption. However, the massive uptake at high relative pressures (above 0.9) cannot be attributed to simple multilayer physical adsorption of water vapor on open surfaces. Desorption branches of the isotherms clearly indicate the presence of an internal pore system which gives rise to a capillary condensation hysteresis loop. Quite obviously there has been a severe alteration of the surface properties. This agrees with our previous result for sample 12070,218 (Holmes *et al.*, 1973) which had been outgassed at 300°C prior to the adsorption of water. Present results show that the reaction of water vapor with these samples does not require prior "activation" at an elevated temperature. It is now apparent that exposure of lunar samples to the normal laboratory atmosphere will result in chemical and physical adsorption of water. Attributing experimental difficulties to adsorbed water is clearly justified (Tittmann *et al.*, 1972). Nitrogen adsorption isotherms on the same sample before and after the reaction with water vapor (Figs. 3 and 4) give a clearer indication of the changes caused by adsorbed water. Obviously the adsorptive capacity has increased by as much as a factor of three. According to de Boer (1958), hysteresis loops such as those in Figs. 3 and 4 are due to either slit-shaped pores with parallel walls or wide pores with narrow necks. The blocking effect of irreversibly adsorbed water (Holmes *et al.*, 1973) favors pores with narrow necks. The isotherms in Figs. 3 and 4 are essentially the same as those reported for 12070,218 (Holmes *et al.*, 1973) and unreported data for 14003,60.

The temperature stability of the water induced porosity has been measured (Figs. 5 and 6). Heating at temperatures of 700 to 800°C eliminates the porosity and markedly reduces the specific surface area (Table 2). This type of sintering behavior is similar to that observed for materials such as some silica-alumina catalysts (Ries, 1952). Significant surface area remained after the 1000°C outgassing (the temperature limit imposed by the microbalance system). One might have expected more drastic sintering on the basis of initial melting temperatures of about 1150°C which have been reported for lunar fines (Gibson and Moore, 1972).

It presently appears that lunar fines, independent of their original location on the lunar surface, will suffer the same general type of alteration by interaction with water vapor at high relative pressures. A common feature to all fines samples is the extensive radiation damage they have suffered. This, the radiation damage, is the basis for our postulated mechanism for the attack by water vapor. According to the "ion explosion spike" model of Fleischer *et al.* (1965), track damage in nonconductors consists of regions of heavy damage ( $\sim 100$  Å) separated by trails of relatively little damage (a few atoms displaced). The damaged material is considerably more soluble than the surrounding material, a fact that has found application in radiation dosimetry (e.g., Becker, 1972) as well as in numerous

studies of radiation damage in lunar samples. We postulate that when sufficient water has been adsorbed (at a relative pressure of about 0.9) the damaged material starts to dissolve. The solution process lowers the vapor pressure of the adsorbed water which leads to increased sorption of water and the entire process is enhanced. Because of the concentration gradient between dissolved material in the damage track and the outer layers of adsorbed water the dissolved material migrates from the damaged region and thereby creates a pore. According to the "ion explosion spike" model the geometry of the pore would be a wide void with a narrow opening. This is one of the two shapes which, according to de Boer (1958), give capillary condensation hysteresis loops like those we observe in nitrogen isotherms on water treated lunar fines. Work in progress should provide further support for this postulated mechanism for the alteration of lunar fines by adsorbed water.

**Acknowledgment**—This research was sponsored by NASA under Union Carbide contract with the U.S. Atomic Energy Commission.

#### REFERENCES

- Becker K. (1972) Dosimetric applications of track etching. *Topics in Radiation Dosimetry*, Suppl. 1, pp. 79-142. Academic Press.
- Brunauer S. (1943) The adsorption of gases and vapors. *Physical Adsorption*, Vol. I. Princeton University Press.
- Brunauer S. (1961) Solid surfaces and the solid-gas interface. *Advances in Chemistry Series*, No. 33, pp. 5-17. American Chemical Society.
- Brunauer S., Emmett P. H., and Teller E. (1938) Adsorption of gases in multimolecular layers. *J. Amer. Chem. Soc.* **60**, 309-314.
- Cadenhead D. A., Wagner N. J., Jones B. R., and Stetter J. R. (1972) Some surface characteristics and gas interactions of Apollo 14 fines and rock fragments. *Proc. Third Lunar Sci. Conf., Geochim. Cosmochim. Acta*, Suppl. 3, Vol. 3, pp. 2243-2257. MIT Press.
- de Boer J. H. (1958) The shapes of capillaries. *The Structure and Properties of Porous Materials* (editors D. H. Everett and F. S. Stone), pp. 68-94. Academic Press.
- Dran J. C., Duraud J. P., Maurette M., Durrieu L., Jouret C., and Legressus C. (1972) Track metamorphism in extraterrestrial breccias. *Proc. Third Lunar Sci. Conf., Geochim. Cosmochim. Acta*, Suppl. 3, Vol. 3, pp. 2883-2903. MIT Press.
- Fleischer R. L., Price P. B., and Walker R. M. (1965) Ion explosion spike mechanism for formation of charged-particle tracks in solids. *J. Appl. Physics* **36**, 3645-3652.
- Fuller E. L., Jr., Holmes H. F., and Secoy C. H. (1965) Gravimetric adsorption studies of thorium dioxide surfaces. *Vacuum Microbalance Tech.* **4**, pp. 109-125. Plenum Press.
- Fuller E. L., Jr., Holmes H. F., Gammage R. B., and Becker K. (1971) Interaction of gases with lunar materials: Preliminary results. *Proc. Second Lunar Sci. Conf., Geochim. Cosmochim. Acta*, Suppl. 2, Vol. 3, pp. 2009-2019. MIT Press.
- Fuller E. L., Jr., Holmes H. F., Gammage R. B., and Secoy C. H. (1972) Gravimetric adsorption studies of thorium oxide, IV. System evaluation for high temperature studies. *Progress in Vacuum Microbalance Techniques*, Vol. 1, pp. 265-274. Heyden and Son.
- Gammage R. B., Fuller E. L., Jr., and Holmes H. F. (1972) Adsorption on porous thorium oxide modified by water. *J. Colloid Interfac. Sci.* **38**, 91-96.
- Gibson E. K., Jr. and Moore G. W. (1972) Thermal analysis-inorganic gas release studies on Apollo 14, 15, and 16 lunar samples. *The Apollo 15 Lunar Samples*, pp. 307-310. The Lunar Science Institute, Houston.

- Gold T., Bilson E., and Yerbury M. (1972) Grain size analysis, optical reflectivity measurements, and determination of high-frequency electrical properties for Apollo 14 lunar samples. *Proc. Third Lunar Sci. Conf., Geochim. Cosmochim. Acta*, Suppl. 3, Vol. 3, pp. 3187-3193. MIT Press.
- Greene C. H., Pye L. D., Stevens H. J., Rase D. E., and Kay H. F. (1971) Compositions, homogeneity, densities, and thermal history of lunar glass particles. *Proc. Second Lunar Sci. Conf., Geochim. Cosmochim. Acta*, Suppl. 2, Vol. 3, pp. 2049-2055. MIT Press.
- Gregg S. J. and Sing K. S. W. (1967) *Adsorption, Surface Area, and Porosity*. Academic Press.
- Grossman J. J., Mukherjee N. R., and Ryan J. A. (1972) Microphysical, microchemical, and adhesive properties of lunar material, III. Gas interactions with lunar material. *Proc. Third Lunar Sci. Conf., Geochim. Cosmochim. Acta*, Suppl. 3, Vol. 3, pp. 2259-2269. MIT Press.
- Holmes H. F., Fuller E. L., Jr., and Secoy C. H. (1968) Gravimetric adsorption studies of thorium oxide, III. Adsorption of water on porous and nonporous samples. *J. Phys. Chem.* 72, 2293-2300.
- Holmes H. F., Fuller E. L., Jr., and Gammage R. B. (1973) Alteration of an Apollo 12 sample by adsorption of water vapor. *Earth Planet. Sci. Lett.* 19, 90-96.
- McClellan A. L. and Harnsberger H. F. (1967) Cross-sectional areas of adsorbed molecules. *J. Colloid Interfac. Sci.* 23, 577-599.
- Phakey P. P., Hutcheon I. D., Rajan R. S., and Price P. B. (1972) Radiation effects in soils from five lunar missions. *Proc. Third Lunar Sci. Conf., Geochim. Cosmochim. Acta*, Suppl. 3, Vol. 3, pp. 2905-2915. MIT Press.
- Ries H. E., Jr. (1952) Structure and sintering properties of cracking catalysts and related materials. *Advances in Catalysis*, Vol. IV, pp. 87-149. Academic Press.
- Smith W. R. and Ford D. G. (1965) Adsorption studies on heterogeneous titania and homogeneous carbon surfaces. *J. Phys. Chem.* 69, 3587-3592.
- Tittmann B. R., Abdel-Gamad M., and Housley R. M. (1972) Elastic velocity and Q factor measurements on Apollo 12, 14, and 15 rocks. *Proc. Third Lunar Sci. Conf., Geochim. Cosmochim. Acta*, Suppl. 3, Vol. 3, pp. 2565-2575. MIT Press.



## Pore Structures Induced by Water Vapor Adsorbed on Nonporous Lunar Fines<sup>1</sup> and Ground Calcite

R. B. GAMMAGE, H. F. HOLMES, E. L. FULLER JR., AND D. R. GLASSON

*Health Physics Division and Reactor Chemistry Division, Oak Ridge National Laboratory, Oak Ridge, Tennessee 37830 U.S.A. and John Graymore Chemistry Laboratories, Plymouth Polytechnic, Plymouth, PL48AA, England*

Received April 25, 1973; accepted May 29, 1973

Lunar fines and the ground calcite are both highly defective materials and because of this there are marked similarities between their interactions with adsorbed water vapor. The solar radiation and meteorites incident on the lunar surface produce soil particles, or fines, which are nonporous to adsorbed inert gas molecules. Many crystalline grains contain very high densities of damage tracks ( $> 10^{11}$  tracks/cm<sup>2</sup>), and show an amorphous coating. The adsorption isotherm of water shows that the fines interact strongly with water vapor. The subsequent adsorptions of nitrogen and argon show that the specific surface area has increased as much as threefold, and that pores have been generated. The probable explanation for these changes is that water interacts with the amorphous coating and diffuses along the damage tracks leaching a system of microchannels.

During the ball milling of calcite the crystals suffer processes of flow and plastic deformation which leave the grains nonporous to adsorbed nitrogen. The structural degradation caused by milling, which was examined by X-ray and infrared techniques, develops in three discrete steps and causes a marked enhancement in the reactivity towards water. The changes in reactivity were examined by measuring the solubility in water, the pH of aqueous suspensions and the buried water content by thermogravimetric analysis. In the most reactive sample of ground calcite, the adsorption isotherm of water reveals massive uptake at high relative pressure and shows high pressure hysteresis overlying a hysteresis which extends over the entire range of relative pressure. The subsequently measured adsorption of nitrogen shows that the grains are now porous and that the specific surface area has increased fourfold. Dissolution occurs within the dislocated calcite to form a pore system of fine channels and crystallization of the leached calcium carbonate forms whiskers of nail-head spar calcite.

### INTRODUCTION

Lunar fines have a history of bombardment by solar and cosmic radiation and meteorites. As a result they are reactive materials with unusual adsorptive properties (1, 2, 3, 4). Calcite ground in a ball mill is a terrestrial material which because of its defective nature displays unusual adsorption characteristics and is highly reactive (5, 6). The purpose of this study is to probe these materials with adsorbed water

and nitrogen molecules and to show how sorbed water drastically modifies the surface characteristics in a manner dependent on the type and extent of structural damage. Despite the widely differing compositions and histories of the lunar fines and the ground calcite, a side by side study reveals a remarkable similarity in their adsorptive properties.

### MATERIALS AND EXPERIMENTAL

Clear crystals of Iceland spar (calcite) were ground in a ball mill made of stainless steel

<sup>1</sup> Research sponsored by NASA under Carbide Contract with the U.S. Atomic Energy Commission.



FIG. 1. 1 MeV dark field electron transmission micrograph showing the nuclear particle tracks and the amorphous coating on a micrometer-sized lunar dust particle (16). The loss of a small grain from the amorphous coat is indicated at A while at B a definite grain surface cementing is seen.

for periods of up to 1000 hr. The amount of contamination by iron was 60 ppm in the 1000-hr sample which indicates only a very small amount of wear. Other details of the milling have been dealt with previously (6). All ground specimens were stored over a desiccant.

Prior to dispatch from the Manned Spacecraft Center the lunar fines were sieved to  $<1$  mm size, the mean particle being about  $100\ \mu\text{m}$  (7). The fines are usually a charcoal grey color and the ones used in this study were part of a contingency sample returned from the

Apollo 12 mission (designated 12070). The samples of fines are encapsulated in vials containing an atmosphere of dry nitrogen. During handling and loading onto the microbalance, however, there is inevitable exposure of the fines to laboratory air.

Adsorption measurements on the ground calcite (5, 6) were made with an electromagnetic sorption balance having a sensitivity of  $10^{-4}$  g (8). Outgassing was carried out at  $150^\circ\text{C}$ . To examine the structural degradation of the calcite the techniques of X-ray diffraction (9), infrared absorption (10), and electron

*Journal of Colloid and Interface Science*, Vol. 47, No. 2, May 1974

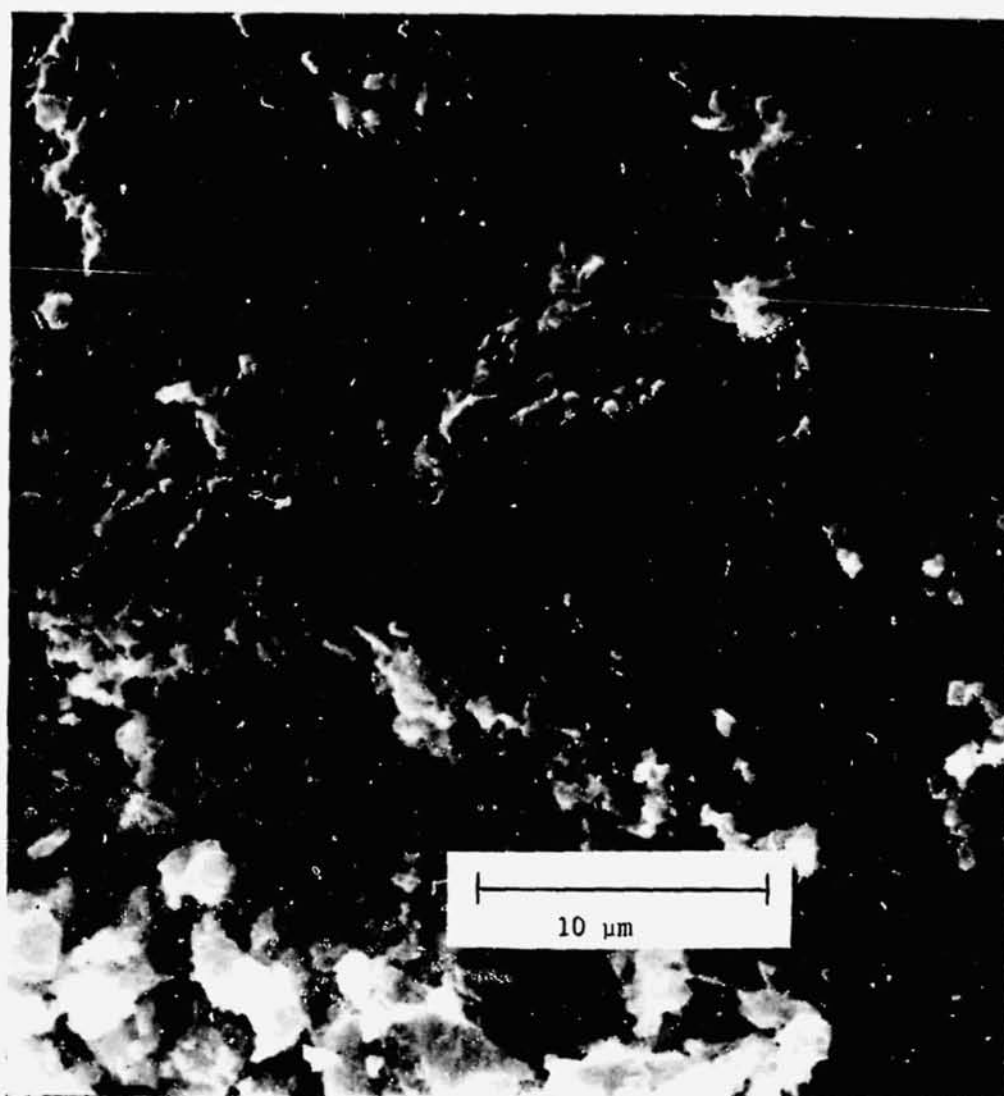


Fig. 2. Scanning electron micrograph of a typical agglutinate found in the Apollo 12 fines (12070) at 4000 magnification.

microscopy (carbon replicas) were employed. The reactivity of the ground calcite was studied by measurements of the solubility in water using the Meigen color test (11) (which relies on the greater solubility of aragonite compared to calcite), by measuring the pH after shaking with water (12) and by determining the water content (buried water taken

up from the air in the milling pot) in a thermogravimetric analysis (13).

Small quantities (400 mg) of the low surface area ( $\sim 0.5 \text{ m}^2/\text{g}$ ) lunar fines were loaded onto a vacuum microbalance of sensitivity  $10^{-6} \text{ g}$  in a vacuum system designed for measuring the adsorption of water vapor and gases such as nitrogen and argon (14). The fines were

*Journal of Colloid and Interface Science*, Vol. 47, No. 2, May 1974



FIG. 3. Scanning electron micrograph of a small glassy area found on a particle from the Apollo 12 fines 12001 at 100,000 magnification.

also examined in a scanning electron microscope at magnifications up to 50,000.

#### RESULTS AND DISCUSSION

##### 1. Lunar Fines: Physical Properties

There is a wealth of information on the physical properties of lunar fines published in the *Proceedings of the First, Second, and Third Lunar Science Conferences* (15). The finest grains extracted from 400 mesh dust residues show the following striking features (16); (a) the proportion of amorphous grains is generally less than 30%; (b) up to 60% of the remaining crystalline grains are surrounded by a superficial layer of amorphous material of thickness  $\sim 500$  Å; (c) 90% of the crystalline grains contain very high densities of latent nuclear particle tracks.<sup>2</sup> The highest track densities

<sup>2</sup> These are damaged regions along the tracks of, in the main, Fe-group ions ( $Z \sim 26$ ) of solar-flare origin. In lunar grains 10  $\mu\text{m}$  in diameter the tracks are randomly oriented and most of them penetrate the entire grain. In the absence of erosions the outer

( $> 10^{11}$  tracks/ $\text{cm}^2$ ) are observed in the rounded grains showing a well-developed and continuous amorphous coating. These features are highlighted in the transmission electron micrographs taken by Borg *et al.* (16), one of which is reproduced in Fig. 1; (d) trapped noble gases from the implantation of solar wind particles are contained within the surface layer to a depth of 2000 Å (18); (e) small grains frequently appear cemented to the surface of coarser rounded and coated grains (see Fig. 1); (f) the amorphous coatings are rapidly soluble under mild etching conditions. This information is most helpful to an understanding of the adsorptive properties and especially to those involving water vapor.

The fragments found in a sample of fines such as sample 12070 can be grouped into (1) glass-coated particles (agglutinates) of the types shown in Figs. 2 and 3; (2) lithic fragments including breccias and discrete mineral

10  $\mu\text{m}$  of a grain would accumulate  $\sim 10^{12}$  Fe-group tracks/ $\text{cm}^2/10^6$  years (17).

*Journal of Colloid and Interface Science*, Vol. 47, No. 2, May 1974

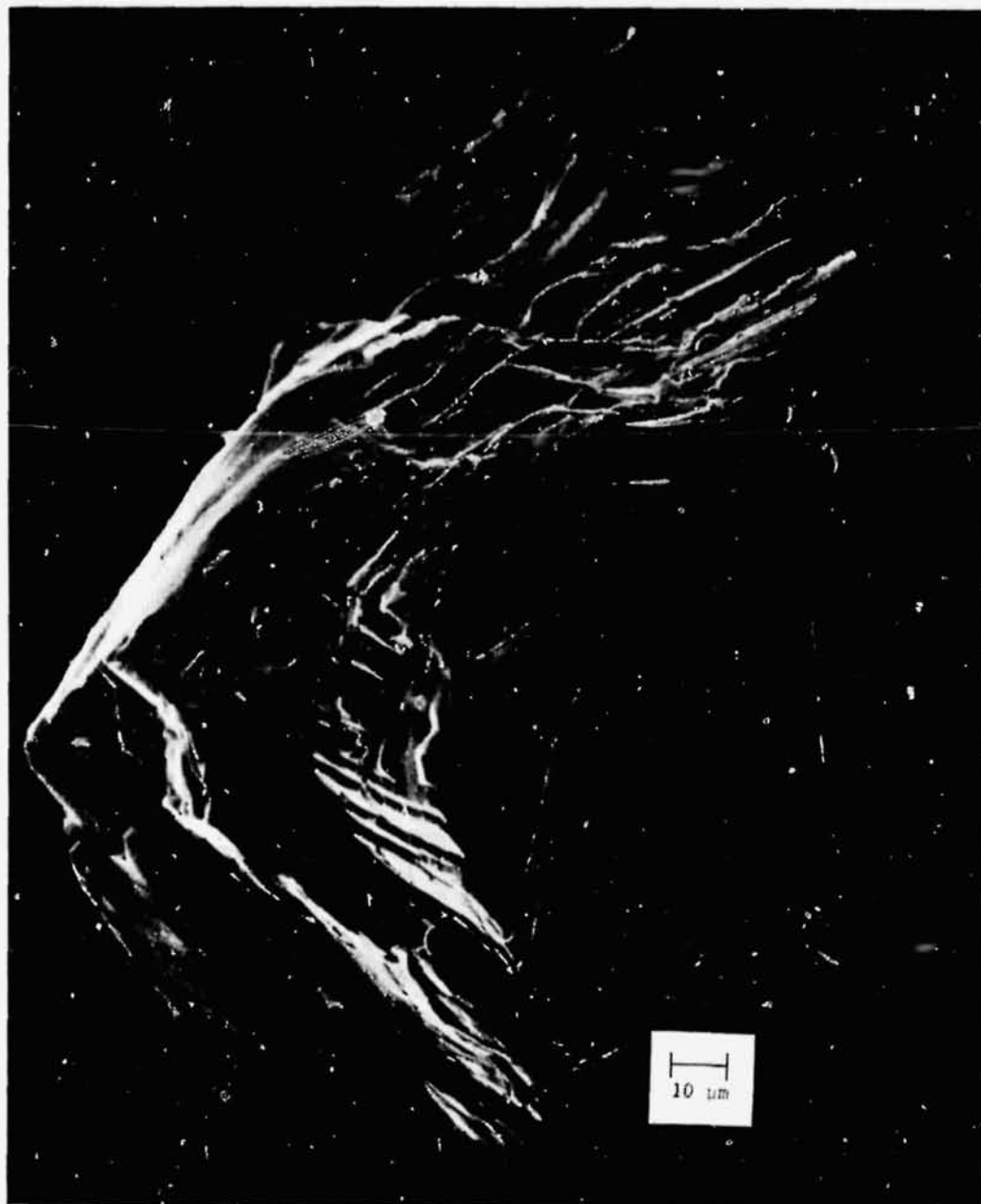


FIG. 4. Scanning electron micrograph of a prismatic crystal of a pyroxene mineral found in the Apollo 12 fines 12070 at 1000 magnification.

fragments of plagioclase (feldspar minerals composed of varying amounts of sodium and calcium aluminum silicate), clino- and orthopyroxene (prismatic crystals of calcium mag-

nesium iron silicate such as the one shown in Fig. 4), and olivine (silicates of magnesium and iron); and (3) a variety of vitric fragments. The major constituents (19) in decreasing

*Journal of Colloid and Interface Science*, Vol. 47, No. 2, May 1974

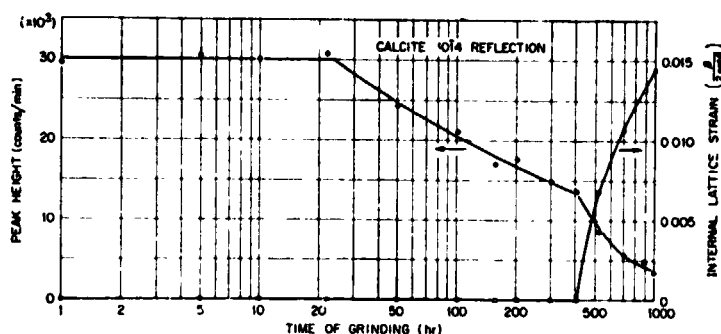


FIG. 5. Loss of characteristically reflected X-ray intensity and line broadening (expressed as lattice strain) in the calcite 1014 reflection as a function of time of grinding.

order of abundance are pyroxene, plagioclase, glass, and olivine. The minor constituents, totaling only a few percent, include ilmenite, tridymite, cristobalite, and nickel-iron.

## 2. Ground Calcite: Structural Degradation

The interaction between ground calcite and adsorbed water and the changes induced in the particles are closely related to the type and extent of structural damage which will now be considered. The results of X-ray diffraction, infrared absorption, and electron microscopy point to a degradation of the calcite occurring in three distinct stages.

There are no significant changes in the X-ray diffraction characteristics of specimens ground for 22 hr and less. Specimens ground for 50 hr and longer gave progressively weaker X-ray lines, the diminution in characteristically reflected intensity for the 1014 reflection being shown in Fig. 5. Broadened lines are produced by specimens ground in excess of 500 hr. The amount of line broadening is expressed, in Fig. 5, as lattice strain. Stage one covers the first 22 hr of milling, the calcite remaining crystalline in both X-ray diffracting properties and appearance (Fig. 6). Stage two covers the period 50 to 500 hr. The crystals flow plastically as is clearly seen in the electron micrograph shown in Fig. 7 and a large quantity of noncrystalline calcium carbonate is produced which reduces the characteristically

reflected X-ray intensity by up to  $\sim 50\%$ . Additionally the deformed calcite is colored blue by the X-ray beam and the unit cell is dilated (e.g., by 0.5% and 1.5% in the 150 hr and 1000 hr samples, respectively). These properties point strongly to the presence of high concentrations of point defects; plastic deformation of ionic crystals generally produces a debris of point defects which are frozen into the crystals (20). In the final 500 hr, stage three, the degradation becomes more severe and the calcite lattice suffers distortion which causes X-ray line broadening.

The infrared absorption spectra shown in Fig. 8 can also be interpreted in terms of structural damage. Absorption occurs at  $878\text{ cm}^{-1}$  and  $861\text{ cm}^{-1}$  in crystalline calcite and aragonite respectively because of differences in the intra-molecular coupling of the out-of-plane bending vibration of the carbonate ion (21). Aragonite appears to be forming in ground calcite, as indicated by the shoulder marked A, even though X-ray diffraction shows that it is absent as a crystalline phase. The pseudo-aragonite is probably a consequence of localized misorientations and strains which force neighboring carbonate ions into positions where the degree of vibrational coupling approximates that found in crystalline aragonite.

The reactivity of the ground calcite reflects the three stages of structural degradation. The solubility (Meigen test) and the buried water

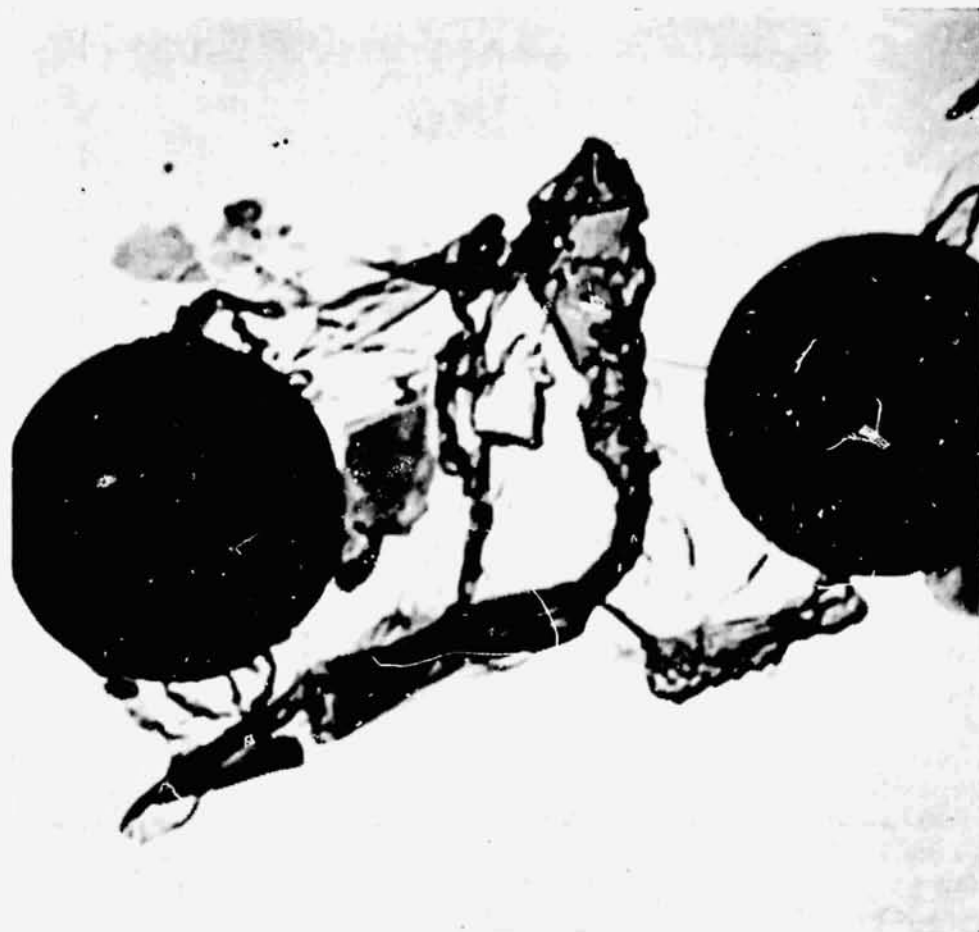


FIG. 6. Electron micrograph of Iceland spar crystals ground for 22 hr; the latex marker beads are  $1.17 \mu\text{m}$  in width.

content,<sup>3</sup> shown as a function of grinding time in Fig. 9, increase in distinct steps corresponding to the onset of plastic deformation at  $\sim 50$  hours and the onset of lattice distortion at  $\sim 500$  hr. The pH, Fig. 10, instead of being enhanced fell sharply at the beginning of stage two. The probable explanation is that hydroxyl ions are removed from solution by the calcite

<sup>3</sup> Water taken up from the air entering the ball mill and becoming tightly bonded and deeply buried within the deformed grains; curves of the fractional weight loss, due to expelled water, per degree rise in temperature show maxima which for the 1000-hr sample occur at  $180^\circ$  and  $300^\circ\text{C}$  at lower temperatures for the calcite ground for shorter times.

which in the disordered state possesses enhanced adsorptive properties. This belief is reinforced by the finding that after annealing the 1000-hr sample and restoring the crystallinity, the pH increases to 10.2 which is within the range of values normally found for crystalline calcite particles.

### 3. Initial Nonporosity

The lunar fines and the ground calcite are nonporous (or nearly so) initially. The isotherms of nitrogen, shown in Figs. 11 and 12, are reversible; usually a nonporous solid gives an isotherm without a hysteresis loop. The



Fig. 7. Electron micrography of Iceland spar crystals ground for 50 hr (0.26  $\mu\text{m}$  latex beads).

lack of porosity is fairly general for lunar fines from different locations on the moon. We obtain isotherms of nitrogen (and argon) without, or with only the slightest trace of, a

hysteresis loop for the fines of Apollo 11 (10087), 12 (12070 and 12001), 14 (14003), and 16 (63341) missions. The Apollo 14 (14163) fines examined by Cadenhead (3) may

*Journal of Colloid and Interface Science*, Vol. 47, No. 2, May 1974



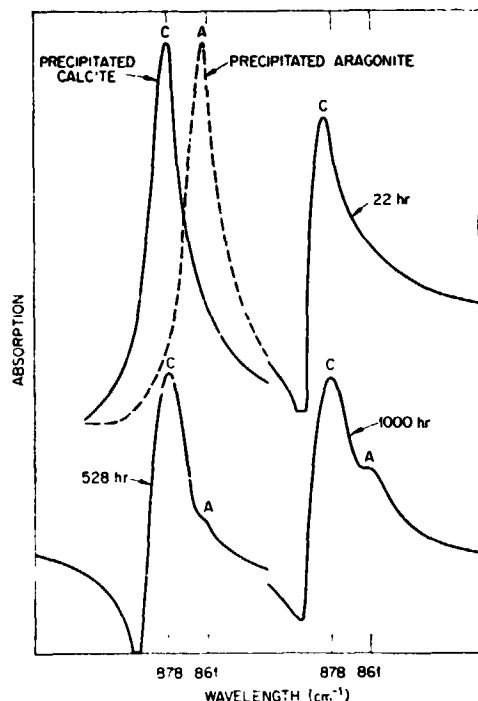


FIG. 8. Infrared absorption spectra of precipitated calcite (C) and aragonite (A) and of Iceland spar ground for 22, 528, and 1000 hr.

be an exception because the physical adsorption isotherm (of water vapor) indicated inherent porosity.

We suggest that the general lack of porosity is due to the combined effects of micrometeorite impact and impinging solar radiation, actions which lead to the filling of interparticle voids and the smoothing of particle surfaces. Impacting micrometeorites cause vaporization and melting and the condensates and splashes produce glassy agglutinates, of the type shown in Figs. 2 and 3, which possess little or no porosity. Micrometeorite bombardment also destroys small particles because they will not survive a collision. Irradiation by solar wind produces the well known amorphous skin, shown in Fig. 1, during the formation of which the particles become smoothed and rounded (16). These processes tend to eliminate any porosity originally present.

The grains of ground calcite have been plastically deformed and welded together (Fig. 7) with the elimination of cracks and pores. The ground calcite is in a Beilby-like state (22). After a crystal of calcite (inorganic crystals in general) has been rubbed or polished the outer few micrometers (23, 24) are composed of a smooth, vitreous-like layer of flowed calcium carbonate—the Beilby layer (22), whose X-ray diffraction properties (25) are the same as those of the ground calcite. Localized frictional heating lends considerable mobility and smoothing power to the surface material (26).

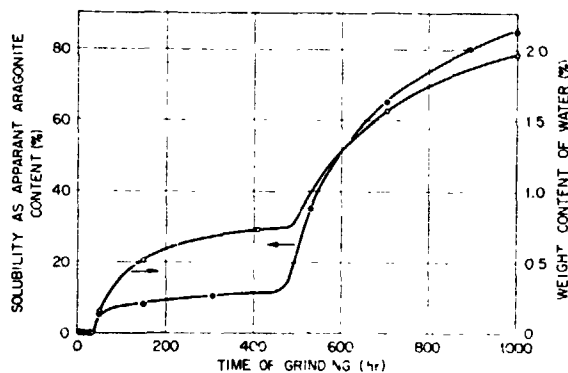


FIG. 9. The solubility, measured by the Meigen color test, as the apparent aragonite content, and the buried water content, determined by thermogravimetric analysis, as a function of the time of grinding the Iceland spar.

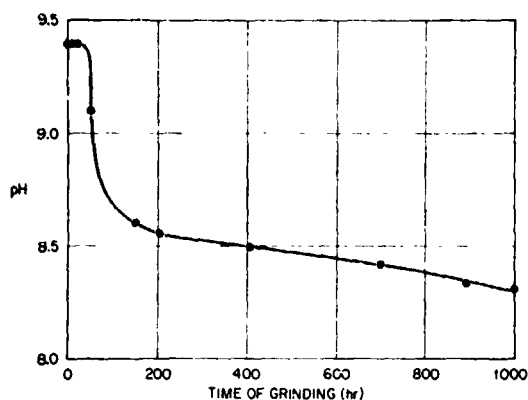


FIG. 10. pH of aqueous suspensions of ground Iceland spar.

#### 4. Adsorption of Water Vapor

The fines sample 12070 chosen for this study shows behavior toward adsorbed water which is typical of several other fines, such as 12001, 14003, and 63341 from the Apollo 12, 14, and 16 missions, on which we have measured the adsorption isotherms of water vapor.

Some fines, such as 10087 (Apollo 11), are more reactive (1) toward water vapor while others, such as 14163 (Apollo 14), are more inert (3). Fines exist, therefore, which cover a range of reactivities with the fines 12070 possessing the median reactivity. Isotherms of water vapor on Iceland spar ground for different

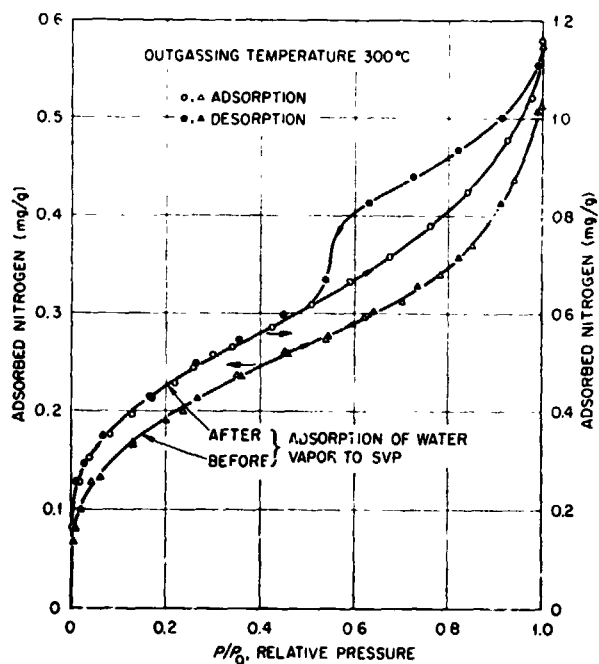


FIG. 11. Adsorptions of nitrogen at 77°K on lunar fines 12070 outgassed at 300°C before and after the adsorption of water vapor.

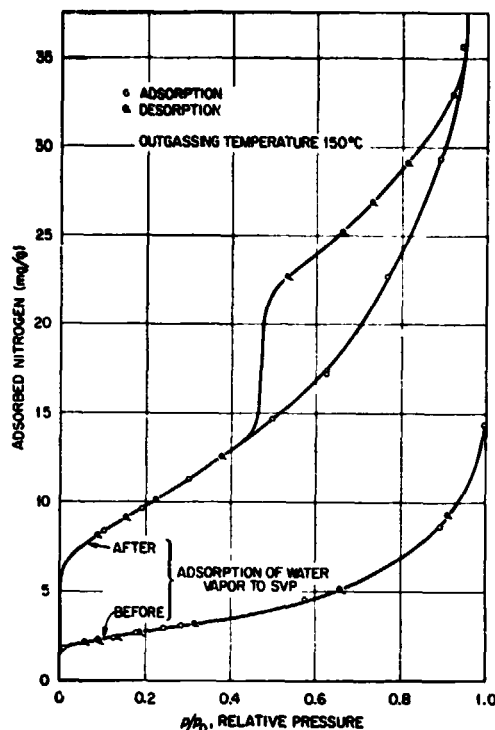


FIG. 12. Adsorption of nitrogen at 77°K on calcite ground for 1000 hr and outgassed at 150°C before and after the adsorption of water vapor.

periods of time have been published elsewhere (6). The calcite ground for 1000 hr is the choice for comparison against the fines 12070 because it is the most severely damaged calcite and the effects of attack by adsorbed water vapor provide the closest resemblance.

Two sorption isotherms of water vapor are shown in Fig. 13 for the lunar fines 12070 and the 1000-hr Iceland spar. Each isotherm shows massive uptake of water at high relative pressure, a general hysteresis extending over the entire range of relative pressure together with additional high pressure hysteresis above  $\sim 0.35 P/P_0$  and the irreversible retention of water, in vacuum, which for the lunar fines is in excess of the amount required for simple chemisorption to form a layer of hydroxyl ions. The massive uptake of water points to water penetrating the bulk of the grains and for the calcite it begins at a lower relative pressure

than for the lunar fines because of the greater solubility of calcite. The high pressure hysteresis shows that pores have been created in both solids.

##### 5. Area Changes and Pores Induced by Adsorbed Water

After completing the adsorptions of water vapor, the isotherms of nitrogen seen in Figs. 11 and 12 were measured. In each material the interaction with water had brought about a drastic change in the surface characteristics. The specific surface area increases from 0.56 to 1.30 m<sup>2</sup>/g and from 7.64 to 28.6 m<sup>2</sup>/g for the lunar fines and ground calcite, respectively. The high pressure hysteresis loops are the result of capillary condensation in pores extending down to a few molecular diameters in size (mesopores). Undamaged terrestrial materials of igneous origin and unground ionic crystals are not changed so drastically

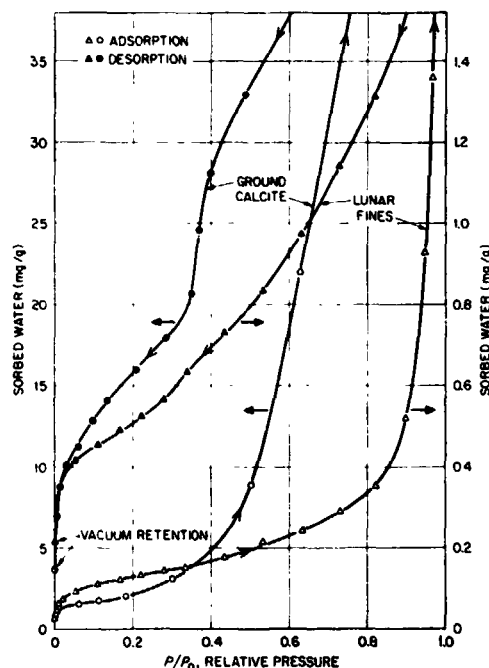


FIG. 13. Isotherms of water adsorbed on lunar fines 12070 at 20°C and 1000-hr calcite at 25°C after outgassing at 300° and 150°C, respectively.

by adsorbed water vapor. Clay type minerals having a layer structure can sometimes be prised open by sorbed polar molecules but minerals with a sedimentary origin are absent from lunar fines. It is because of their damaged natures that the lunar fines and the ground calcite are similar in their adsorptive properties and are different from other undamaged terrestrial materials.

The adsorption data have been analysed by the thickness or  $t$ -plot method developed by de Boer (27) in which the amount of adsorbed nitrogen is compared to the thickness of the adsorbed nitrogen layer on a reference nonporous solid. For this study the adsorptions of nitrogen on the nonporous lunar fines and the nonporous ground calcite conveniently provide the reference data. The resulting  $t$ -plots with a summary of the analyses are shown in Fig. 14 and Table I. The linear section of the  $t$ -plot is displaced vertically upwards by nitrogen adsorbed in micropores ( $< \sim 20$  Å width). The intercept is a measure of the micropore volume (or apparent micropore area  $S_m$ ) and the gradient of the straight line is a measure of the area  $S_t$  contained in larger mesopores ( $\sim 20$  to  $\sim 200$  Å in width) and on the open surface. The close correspondence between  $S_t + S_m$  and  $S_{BET}$ , the specific surface area calculated by the BET method, indicates that our reference isotherms are the appropriate ones to use. We have successfully followed the advice given in an earlier paper (28) that the

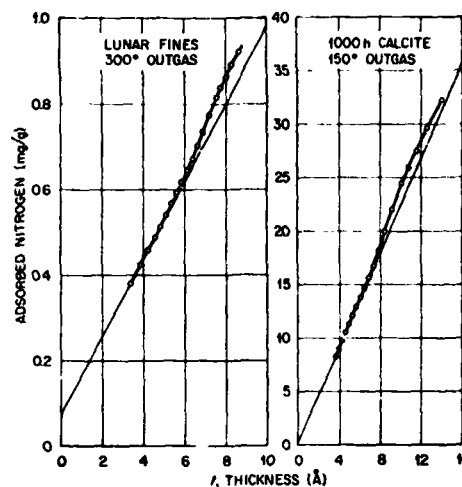


FIG. 14.  $t$ -plot for the adsorption of nitrogen on lunar fines 12070 and 1000-hr calcite which had been exposed to water at saturation vapor pressure.

oxide (or calcite) used to obtain the reference isotherm should preferably be of the same type as the experimental oxide (or calcite) and of course, be nonporous. After the adsorption of water vapor the lunar fines contain smaller pores than the ground calcite; the apparent micropore area is proportionately much higher in the fines (19% compared to 3.5%) and the  $t$ -plot begins to deviate upwards from the linear section at a smaller  $t$ -value.

The standard nitrogen adsorption data for the nonporous lunar fines are listed in Table II.

TABLE I  
SUMMARY OF  $t$ -PLOT ANALYSES OF NITROGEN ADSORPTION DATA

Sample	OGT (°C)	$S_{BET}$ (m <sup>2</sup> /g)	C constant	C constant for refer- ence iso- therm	$S_t$ (m <sup>2</sup> /g)	$S_m$ (m <sup>2</sup> /g)	$S_t + S_m$ (m <sup>2</sup> /g)	$S_t + S_m$ $S_{BET}$
Lunar fines 12070 after sorption of water	300	1.30	92	43	1.12	0.26	1.38	1.06
1000-hr calcite after sorption of water	150	28.6	101	106	27.3	1.0	28.3	0.99

TABLE II  
VALUES OF  $n$  AND  $t^*$  FOR NITROGEN ADSORBED  
ON NONPOROUS LUNAR FINES 12070

$P/P_0$	$n$	$t^*$
0.10	0.95	3.37
0.15	1.08	3.82
0.20	1.19	4.21
0.25	1.29	4.56
0.30	1.37	4.86
0.35	1.44	5.10
0.40	1.52	5.36
0.45	1.59	5.62
0.50	1.66	5.89
0.55	1.74	6.15
0.60	1.81	6.41
0.65	1.88	6.65
0.70	1.96	6.93
0.75	2.04	7.23
0.80	2.14	7.58
0.825	2.20	7.77
0.85	2.27	8.04
0.875	2.35	8.32
0.90	2.46	8.71

\*  $t = 3.54 n$ , where  $n$  is the number of adsorbed layers each of thickness 3.54 Å (27).

Compared to reference isotherm data for nonporous terrestrial oxide samples published by, for example, Pierce (29) and Sing (30), a significantly smaller amount of nitrogen is adsorbed above 0.5  $P/P_0$  on the lunar fines. Additional measurements of adsorbed nitrogen on a wider range of lunar fines should tell us whether or not this difference between the standard isotherms for terrestrial and lunar oxide samples is general.

#### 6. Porosity Related to Structural Damage

The appearance of fine channels in the 1000-hr calcite is fairly easy to explain. The structure contains a high concentration of point defects and dislocations which cause distortion of the lattice by  $\sim 1.5\%$  (Fig. 5). Adsorbed water diffuses along fault lines with dissolution of the dislocated calcite to form a pore system of fine channels. The dissolved calcium carbonate crystallizes to form whiskers of nail-head spar calcite on the surface of the grains. These micrometer-sized crystals are clearly

visible in the electron micrograph shown in Fig. 15. All the other tests involving water (solubility, pH, and buried water content) confirm the enhancement of reactivity.

The hysteresis loop in the nitrogen isotherm (1000-hr calcite) is similar to a Type B hysteresis loop [classification of de Boer (31)] which is obtained characteristically for a pore system of narrowly separated parallel plates. It is visualized that dissolution of calcium carbonate within the walls of dislocation forms such a system of slit-shaped pores. The sudden closure of the hysteresis loop at  $\sim 0.45 P/P_0$  indicates a plate separation of about 36 Å as calculated by methods based on the Kelvin equation (32).

There is evidence, from small angle X-ray scattering studies, that along the track left by a nuclear particle traversing an inorganic crystal, the damaged region varies in width (33). If in the lunar fines the water diffuses into and leaches material out of the damage regions of nuclear particle tracks then one might anticipate a tubular system of pores with narrow constrictions between the wider parts. The studies discussed in this paper show only that micro- and mesopores are produced. Our current investigations, to be published in the *Proceedings of the Fourth Lunar Science Conference* point strongly towards a tubular pore system; by using outgassing temperatures lower than the 300°C used in this study, entry of nitrogen to the mesopores is partially prevented by molecular water bound within the narrow constrictions. At 300°C all of this water is removed and the pore system has maximum accessibility.

#### SUMMARY

Adsorptions of nitrogen show that the lunar fines and the ground calcite are initially nonporous. Vaporization, condensation, melting, and splashing events during meteorite impact cause interparticle voids to be filled and the smoothing of surfaces. Irradiation by solar wind particles also smooths and rounds the particles. The grains of ground calcite are devoid of pores because of flow and welding



FIG. 15. Electron micrograph of 1000-hr calcite after treatment with water vapor, showing the whiskers of nail-head spar (0.26  $\mu$ m latex heads).

processes which occur during plastic deformation in the ball mill.

Both materials exhibit a high reactivity toward water vapor. This is because of amorph-

*Journal of Colloid and Interface Science*, Vol. 47, No. 2, May 1974

ous surface layers and high densities of nuclear particle damage tracks in the lunar fines and because of a severely dislocated structure in the ground calcite which has a high concentration of point defects and a distorted crystal lattice. Particles of the lunar fines and the ground calcite are "opened up" by the action of adsorbed water vapor; leaching causes the specific surface area to increase several fold and a system of pores to develop. Crystallization of the calcium carbonate dissolved from the region of fault lines gives whiskers of nail-head spar calcite. The data from adsorptions of nitrogen suggest that the lunar fines contain tubular pores with narrow constrictions (micropores) formed along damage tracks. The pore system in the ground calcite is more open, the capillary condensation behavior suggesting the presence of slit-shaped openings of width  $\sim 36 \text{ \AA}$ .

#### ACKNOWLEDGMENTS

The authors (and particularly R. B. Gammage) wish to thank Dr. S. J. Gregg for his guidance of the studies with ground calcite and offer their appreciation to Professor P. H. Emmett for stimulating discussions on the studies with lunar fines.

#### REFERENCES

1. FULLER, JR., E. L., HOLMES, H. F., GAMMAGE, R. B., AND BECKER, K., *Proc. Second Lunar Sci. Conf., Geochim. Cosmochim. Acta, Suppl. 2*, 3, 2009 (1971).
2. HOLMES, H. F., FULLER, JR., E. L., AND GAMMAGE, R. B., *Earth and Interplanetary Sci. Lett.* 19, 90 (1973).
3. CADENHEAD, D. A., WAGNER, N. J., JONES, B. R., AND STETTER, J. R., *Proc. Third Lunar Sci. Conf., Geochim. Cosmochim. Acta, Suppl. 3*, 3, 2243 (1972).
4. GROSSMAN, J. J., MUKHERGEE, N. R., AND RYAN, J. A., *Proc. Third Lunar Sci. Conf., Geochim. Cosmochim. Acta, Suppl. 3*, 3, 2259 (1972).
5. GAMMAGE, R. B., Ph.D. Thesis, Exeter University, England (1964).
6. GAMMAGE, R. B., AND GREGG, S. J., *J. Colloid Interface Sci.* 38, 118 (1972).
7. "The Apollo 16 Lunar Samples: A Petrographic and Chemical Description of Samples from the Lunar Highlands by the Apollo 16 Preliminary Examination Team," Manned Spacecraft Center, Houston, Texas (1972).
8. GREGG, S. J., *J. Chem. Soc.*, 1438 (1955).
9. ADAMS, L. H., AND ROWE, F. A., *Amer. Min.* 39, 215 (1954).
10. BONHAM, L. C., HUNT, J. M., AND WISHERD, M. P., *Indust. Chem. Eng., Anal. Sec.* 22, 1478 (1950).
11. SMITH, M. L., *J. Soc. Chem. Indust.* 16, 283T (1937).
12. STURGE CO., England, Technical Leaflet No. 2, "The Chemical Analysis of Precipitated Calcium Carbonate."
13. NEWKIRK, A. E., *Anal. Chem.*, 1558 (1960).
14. FULLER, JR., E. L., HOLMES, H. F., AND SECOY, C. H., *Vac. Microbalance Tech.* 4, 109 (1965).
15. *Proc. of the First, Second, and Third Lunar Sci. Conf., Geochim. Cosmochim. Acta*, MIT Press, 1970-72.
16. BORG, J., MAURETTE, M., DURRIEU, L., AND JOURET, C., *Proc. Second Lunar Sci. Conf., Geochim. Cosmochim. Acta, Suppl. 2*, 3, 2027 (1971).
17. BARBER, D. J., COWSIK, R., HUTCHESON, I. D., PRICE, P. B., AND RAJAN, R. S., *Proc. Second Lunar Sci. Conf., Geochim. Cosmochim. Acta, Suppl. 2*, 3, 2705 (1971).
18. EBERHARDT, P., GEISS, J., GRAF, H., GRÖGLER, N., KRÄHENBÜHL, U., SCHWALLER, H., SCHWARZMÜLLER, J., AND STETTLER, A., *Science* 167, 558 (1970).
19. "Apollo 12 Lunar Sample Information Catalog," p. 56. Lunar Receiving Laboratory, Manned Spacecraft Center, Houston, Texas, January 12, 1970.
20. VAN BUEREN, H. G., "Imperfections in Crystals," Chapter 27. North-Holland Pub., Amsterdam; Interscience Pub. New York, 1960.
21. DECIUS, J. C., *J. Chem. Phys.* 22, 1946 (1954).
22. BEILBY, G., "Aggregation and Flow in Solids." MacMillan, London, 1921.
23. HOPKINS, H. G., *Phil. Mag.* 21, 820 (1936).
24. FINCH, G. I., *Trans. Faraday Soc.* 33, 425 (1937).
25. EVANS, R. C., HIRSCH, P. B., AND KELLER, J. N., *Acta Cryst.* 1, 124 (1948).
26. BOWDEN, F. P., AND TABOR, D., "The Friction and Lubrication of Solids," Chapter 3, Clarendon Press, Oxford, 1950.
27. LIPPENS, B. C., LINSSEN, B. G., AND DE BOER, J. H., *J. Catal.* 3, 32 (1964).
28. GAMMAGE, R. B., FULLER, JR., E. L., AND HOLMES, H. F., *J. Colloid Interface Sci.* 38, 91 (1972).
29. PIERCE, C., *J. Phys. Chem.* 72, 3673 (1968).
30. SING, K. S. W., *Chem. Ind. (London)*, 918 (1969).
31. DE BOER, J. H., "The Structure and Properties of Porous Materials," p. 68. Butterworth, London, 1958.
32. GREGG, S. J., AND SING, K. S. W., "Adsorption Area and Porosity," p. 162. Academic Press, London, 1967.
33. LAMBERT, M., LEVELU, A. M., MAURETTE, M., AND HECKMAN, H., *Jour. Int. d'Enreg. des Traces dans les Solides Isolants*, Clermont-Ferrand, 1969.